Electromechanical Energy Conversion Systems (EECS)
Niroo Research Institute (NRI)
Vol. 4, No. 2, Summer 2025, pp. 8-34
DOI: 10.30503/eecs.2025.488806.1065
Original Article

Magnetic Force Calculation Using Lorentz Force and Energy Conservation in Electrical Machines

Mohammad Hosein Javanmardi[1*], Akbar Rahideh[1], and Jafar Rouzegar[2]

Abstract

In many engineering textbooks, very simple algebraic relations are used for magnetic forces. The simplicity of the relations lies in the well-known magnetic circuit model from which they have been derived. However, some applications require more accuracy. One niche application is the calculation of magnetic forces in electrical machines due to the slotting effect. The application is twofold: 1) *vibration analysis* which requires calculation of the net torque ripple (leading to cogging torque) and the oscillation of resultant normal force (attractions/repulsions). 2) *deformation analysis* which requires calculating the surface and volume force density distribution. Given the magnetic field distribution, the analyses can be furnished by leveraging advanced formulae of magnetic force. Thus, in order to increase the accuracy, engineers would have to resort to 1) more advanced magnetic models that yield a precise two-dimensional magnetic field distribution and 2) a reliable method of magnetic force calculation. The latter is the subject of this paper. To be a reference for the engineering community, this paper follows these objectives: 1) since not all engineers are accustomed with advanced physics topics, this paper aims to bring a handful of formulae from the outset. Additionally, two novel formulae are derived: *surface force density* and *Maxwell couple stress tensor*. 2) Revisiting the underlying theory and derivation of the related formulae for three purposes: 2-1) providing subjective foresight, 2-2) elucidating the limitations of the usage of the formulae, and 2-3) to point out common mistaken interpretations. Two case studies are investigated to verify the identity of all formulae.

Keywords: analytical model, Maxwell stress tensor, vibration, deformation, virtual work.

Received Date: 2024-11-14; Revised Date: 2025-03-18; Accepted Date: 2025-09-16

1. INTRODUCTION

Forces and energies are intimately connected physical quantities and are of utmost importance in designing electrical machines. At the initial design, a rough conception of the force creation seems sufficient and very simple formulas can be employed. The approximate method can be a simple lumped model such as winding function or magnetic circuit methods. But in advanced modeling techniques such as the separation of variables method (SVM), integral equation methods and finite element method (FEM), a two-dimensional (2-D) or three-dimensional (3-D) field distribution is derived. In such cases, the designer should have deep insight into the magnetostatic field interactions leading to the generation of electromagnetic forces. As a result, more accurate formulas must be used. Unfortunately, in the literature, this important matter has not been deeply discussed. Discussions arise for both concept and computation.

Since FEM is formulated based on potential energy minimization, FEM users usually use co-energy to obtain electromagnetic forces. However, the quality of the air-gap discretization impacts not only the computational cost, but also the accuracy; therefore, special numerical treatment is required. For instance, in [1], different approaches to force calculation for FEM have been discussed and compared. It is concluded that a hybrid numerical method called the nodal force method that combines the Maxwell stress and virtual work methods is accurate and efficient in FEM [2]. In [3], a modified form of Maxwell stress is proposed that does not have the inaccuracy of its raw form for FEM usage. In order to mitigate the air-gap discretization effect, in [4], FEM is hybridized with SVM in the air gap to improve the accuracy of the Maxwell stress method. This method is called the *stress harmonic filter* by the author, since it filters out the harmonics of the magnetic field distribution obtained from FEM. The method solves the air-gap field distribution through a boundary value problem using SVM and harmonic analysis.

Having known the effectiveness of Fourier analysis and also the familiarity of the engineering community with this subject, SVM models have been vastly investigated.

[1] *Department of Electrical Engineering, Shiraz University of Technology*
[2] *Department of Mechanical Engineering, Shiraz University of Technology*
**Corresponding author: m.hosein.javanmardi@gmail.com*

Calculation of force is then performed using Maxwell stress method [5], [6], [7], [8] ,[9] ,[10] ,[11], but none of them have reported the principal considerations. If these are not truly understood, it may often lead to a misleading perception of the concept of *magnetic force*. In such cases, accurate solutions might be obtained, however, with an incorrect implementation. For example, Maxwell stress may depend on the radius of the integration path in the air gap [12], while theoretically, it should not be.

The contents of this paper are as follows,

1. Introduction
2. Force density
3. Virtual Stresses
4. Resultant (Net) Force
5. Energy Method
6. Application in Rotating Machines
7. Application in Mechanical Design
8. Fundamental Questions
9. Validation and Case-study
10. Summary and Concluding Remarks

The introductory principles are reviewed in sections 2-5. Some new formulas are meanwhile derived. Among them, the boldest ones are 1) the *magnetic surface force density* and 2) the *magnetic couple stress*. The key formulae are boxed to attract the readers grasp. In Section 6, the formulas are simplified in the application of electrical machines with a focus on Harmonic models. Section 7 gives a brief on the application of the formulas in mechanical design. In Section 8, some theoretical misperceptions are pointed out in the form of answered questions. Some of the important formulae are validated in Section 9 through two case studies: 1) a conceptual machine that has a closed-form solution, and 2) a more realistic machine using FEM simulation.

2. Force Density

In this section, the concept of force density is described using the Lorentz force law.

Lorentz Force Law

The Lorentz force law, which is proved in practice through experiment, combined with Maxwell equations, forms the foundations of classical electromagnetism [13]. It states that a point charge dq moving with velocity $\mathbf{v}$ in a magnetic field $\mathbf{B}$ experiences a magnetic force $d\mathbf{F}$,

$$d\mathbf{F} = dq\mathbf{v} \times \mathbf{B}$$

The differential term $dq\mathbf{v}$ is of a single traveling point charge. This concept can easily be extended to a continuous charge distribution flowing along a line, on a surface or within a volume,

$$dq\mathbf{v} = \mathbf{I}dl = \mathbf{J}_s ds = \mathbf{J}_v dv$$

where dl, ds and dv are the differential elements of respectively line, surface and volume. This creates current $\mathbf{I}$, surface current density $\mathbf{J}_s$ and volume current density $\mathbf{J}_v$. The differential force $\mathbf{dF}$ is therefore restated as

$$d\mathbf{F} = dq\mathbf{v} \times \mathbf{B} = \mathbf{I}dl \times \mathbf{B} = \mathbf{J}_s ds \times \mathbf{B} = \mathbf{J}_v dv \times \mathbf{B}$$

Dividing the expressions by the differential elements yields:

- *linear force density* $\mathbf{f}_l$, i.e. the force per unit length

$$\mathbf{f}_l = \frac{d\mathbf{F}}{dl} = \mathbf{I} \times \mathbf{B} \quad (1)$$

- *surface force density* $\mathbf{f}_s$, i.e. the force per unit area

$$\mathbf{f}_s = \frac{d\mathbf{F}}{ds} = \mathbf{J}_s \times \mathbf{B} \quad (2)$$

- *volume force density* $\mathbf{f}_v$, i.e. the force per unit volume

$$\mathbf{f}_v = \frac{d\mathbf{F}}{dv} = \mathbf{J}_v \times \mathbf{B} \quad (3)$$

The force density is a distribution, i.e. it is a vector field which assigns a vector to each point of a body.

Important note

1) The surface current density of a volume-distributed current is zero:

$0<\mathbf{J}_v<\infty \rightarrow \mathbf{J}_s=0$;

because,

$$\mathbf{J}_s = \frac{d\mathbf{I}}{dw} = \frac{d\mathbf{I}}{ds}\frac{ds}{dw} = \mathbf{J}_v dh = 0$$

2) The volume current density of a surface-distributed current is not bounded:

$0<\mathbf{J}_s<\infty \rightarrow \mathbf{J}_v=\infty$;

because,

$$\mathbf{J}_v = \frac{d\mathbf{I}}{ds} = \frac{d\mathbf{I}}{dw} / \frac{ds}{dw} = \frac{\mathbf{J}_v}{dh} = \infty$$

where dl, dw, and dh are respectively the differential elements of length, width and height of the differential volume element dv. The current passes along the length (Fig. 1).

$ds = dh\, dw$

$dv = ds\, dl$

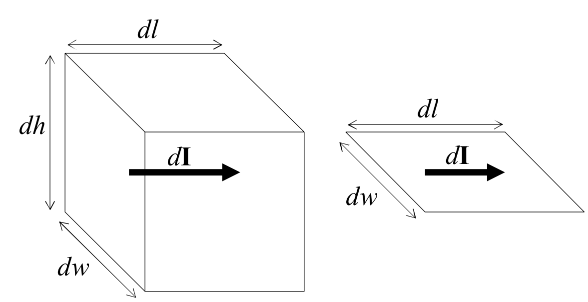

Fig. 1. Volume current density in a volume element (left) and surface current density on a surface element (right).

Remark: According to the above note, a finite nonzero value of surface current density exists for a *current sheet* and a finite nonzero volume current density exists for a *bulk current*. By this virtue, each definition of force density makes sense for only the associated current density. For instance, volume force density corresponds to only volume current density.

Remark: The Lorentz force law does indeed contain another term $\rho\mathbf{E}$ which indicates the contribution of electrostatic field. Since this paper is devoted to electrical machines, only the magnetic part is considered.

Remark: The volume force density **f** is sometimes notated with **p** [14], however **p** is usually the notation of pressure. Therefore in here, the usual notation **f** is adopted [15]. It is noted that the capital letter **F** indicates the total force as opposed to small letter **f** which denotes the force density.

In some cases, the current density **J** is not explicitly known. One instance is regarding ferromagnetic materials. Therefore, it is more convenient to express (2) and (3) purely in terms of magnetic field. It is noted that the linear force density (1) corresponds only to a single current-carrying wire. Current density is not defined for a wire and the current **I** is usually a known current.

Surface Force Density

The presence of surface current density creates a discontinuity in the tangent component of the magnetic field with respect to the surface of the current sheet. It is shown [13] that the field discontinuity is governed by the following magnetostatic boundary condition,

$$\mathbf{a}_n \times (\mathbf{B}_1 - \mathbf{B}_2) = \mu_0 \mathbf{J}_s \tag{4}$$

where μ_0 is the magnetic permeability of vacuum. In the above relation, the unit vector $\mathbf{a}_n$ is normal to the surface of current and in the direction pointing from side "2" to side "1" (Fig. 2).

The relation (4) provides a way to rewrite the Lorentz force law (2) only in terms of the magnetic field. However, there is another problem. The existence of discontinuity in the magnetic field infers that **B** is vague in (2). Even with this ambiguity, a unique surface force density exists for each point on the surface of a current sheet, which is derived in the following.

Consider an infinitesimal element of surface ds on the current sheet. The surface force density on ds, is indeed the force exerted from all sources of magnetic field in the surrounding, except for the ds itself. That is because ds cannot exert force on itself. Therefore, the total magnetic field **B** in (2) can be replaced with the external magnetic field $\mathbf{B}_{ext}$. Fortunately, $\mathbf{B}_{ext}$ is continuous and, unlike **B,** has a unique value. It is proved in Appendix 1-Theorem (1) that for a current sheet, $\mathbf{B}_{ext}$ is the mean value of **B**.

$$\mathbf{B}_{ext} = \frac{1}{2}(\mathbf{B}_1 + \mathbf{B}_2) \tag{5}$$

The surface force density can now be obtained by means of only the knowledge of the total magnetic field by substituting (4) and (5) in (2),

$$\mathbf{f}_s = \frac{1}{2}\mu_0^{-1}(\mathbf{a}_n \times (\mathbf{B}_1 - \mathbf{B}_2)) \times (\mathbf{B}_1 + \mathbf{B}_2) \tag{6}$$

In case of 2-D field distribution, this formula can be expressed simpler in a t-n frame, i.e. a local right-handed coordinate system whose t-axis is tangent to the surface and whose n-axis is normal to the surface (Fig. 2).

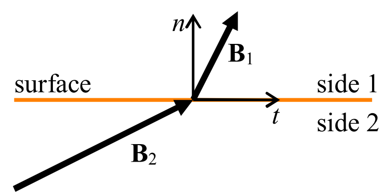

Fig. 2. Depiction of flux density discontinuity at the surface of a current sheet.

The flux density can be written in terms of the t-n components,

$$\mathbf{B} = B_t\mathbf{a}_t + B_n\mathbf{a}_n = \begin{bmatrix} B_t \\ B_n \end{bmatrix}$$

where $\mathbf{a}_t$ and $\mathbf{a}_n$ are the unit coordinate vectors. From (6), it follows that

$$\mathbf{f}_s = \frac{1}{2}\mu_0^{-1}(\mathbf{a}_n \times (\mathbf{B}_1 - \mathbf{B}_2)) \times (\mathbf{B}_1 + \mathbf{B}_2)$$

$$\begin{bmatrix} f_{s,t} \\ f_{s,n} \end{bmatrix} = \frac{1}{2}\mu_0^{-1}\begin{bmatrix} 0 \\ 1 \end{bmatrix} \times \begin{bmatrix} B_{1,t} - B_{2,t} \\ B_{1,n} - B_{2,n} \end{bmatrix} \times \begin{bmatrix} B_{1,t} + B_{2,t} \\ B_{1,n} + B_{2,n} \end{bmatrix}$$

$$\begin{bmatrix} f_{s,t} \\ f_{s,n} \end{bmatrix} = \frac{1}{2}\mu_0^{-1}\begin{bmatrix} (B_{1,t} - B_{2,t})(B_{1,n} + B_{2,n}) \\ -(B_{1,t} - B_{2,t})(B_{1,t} + B_{2,t}) \end{bmatrix}$$

It is a fact that the normal component of magnetic flux density is continuous ($B_{1,n}$=$B_{2,n}$) [13], thus, by definition of B_n as

$$B_n = \frac{1}{2}(B_{1,n} + B_{2,n})$$

and a simplification is obtained as follows,

$$\begin{bmatrix} f_{s,t} \\ f_{s,n} \end{bmatrix} = \begin{bmatrix} \mu_0^{-1}(B_{1,t} - B_{2,t})B_n \\ -\frac{1}{2}\mu_0^{-1}(B_{1,t}{}^2 - B_{2,t}{}^2) \end{bmatrix} \tag{7}$$

It is reminded that the n-direction is the outwards side "2" and towards side "1".

In the special case where

- no free current runs at the surface,
- side "1" refers to a nonmagnetic medium (such as air) and
- side "2" refers to a perfectly permeable ferromagnetic medium (μ^{-1}=0),

the magnetic field in side "1" enters completely perpendicular to side "2", i.e. $B_{1,t}$ =0. In this case, (7) simplifies as follows,

$$\begin{bmatrix} f_{s,t} \\ f_{s,n} \end{bmatrix} = \begin{bmatrix} -\mu_0^{-1} B_{FM,t} B_n \\ \frac{1}{2}\mu_0^{-1} B_{FM,t}^{\ 2} \end{bmatrix} \tag{8}$$

where $B_{FM,t}$ refers to the tangent component of magnetic field in the ferromagnetic side and n-direction is outwards the ferromagnetic medium.

Volume Force Density

In order to rewrite the volume force density (3) only in terms of magnetic field, Maxwell equations are involved with Lorentz force law. Ampere's law reads as,

$$\nabla \times \mathbf{B} = \mu_0 \mathbf{J} \tag{9}$$

Substituting (9) in (3) yields

$$\mathbf{f}_v = \mu_0^{-1}(\nabla \times \mathbf{B}) \times \mathbf{B} \tag{10}$$

Alternatively, (10) can also be expanded as follows (proof in Appendix 2 - Theorem (3)),

$$\mathbf{f}_v = \mu_0^{-1}\left((\mathbf{B}\cdot\nabla)\mathbf{B} - \frac{1}{2}\nabla|\mathbf{B}|^2\right) \tag{11}$$

The two resulting terms in the above expansion are named the *tension force* and the *pressure gradient force*, respectively (Fig. 3).

- The tension force resembles a part of force that appears for curved flux lines. It tends to straighten the bent flux lines.
- The pressure gradient force represents the portion due to the variation of the flux density magnitude. It points from areas with high flux density to low flux density regions.

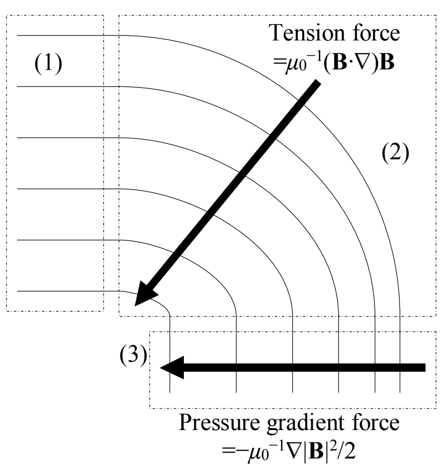

Fig. 3. Force generation by variation of flux lines. 1) The field lines are uniform thus no force arises. 2) The field lines are bent and a tension force appears that tends to straighten them. 3) The flux lines are more intense in some regions; thereby a force is generated that is directed towards low flux density areas.

These concepts are mainly used in the context of plasma physics and magneto-hydrodynamics and not in electrical machines. By neglecting the hydrostatic pressure and considering only the electromagnetic force, these concepts are reduced to the context of electrical machines [24].

These components of magnetic force density can be simplified using the knowledge that the force is perpendicular to magnetic field (because of the vector product in $\mathbf{f}=\mathbf{J}\times\mathbf{B}$) [24]. In that, local t-n frame on magnetic flux lines should be imposed. However, the simplified form requires calculating the curvature of flux lines. There are two methods for this purpose:

1) Extrapolating the direction of flux density $\mathbf{B}$,
2) Creating the graph of equipotential lines of magnetic vector potential A_z (only in 2-D).

Field lines are mainly used for visualization not numerical computation; therefore more study is required in this approach.

Although relations (10) and (11) seem sufficient, a few manipulations would greatly simplify further computations, as will be shown in the next section.

Torque Density

By virtue of the concept of volume force density $\mathbf{f}_v$, it is possible to define volume torque density $\boldsymbol{\tau}_v$,

$$\boldsymbol{\tau}_v = \frac{d\mathbf{T}}{dv} = \mathbf{r} \times \mathbf{f}_v \tag{12}$$

where $d\mathbf{T}$ is the differential torque exerted to volume element dv located at a point with location vector $\mathbf{r}$. The torque density is a vector, however the definition for any component can easily be extended. The axial component is illustrated in Fig. 4.

Using (3), the torque per unit volume reads as follows,

$$\boldsymbol{\tau}_v = \mathbf{r} \times (\mathbf{J}_v \times \mathbf{B}) \tag{13}$$

The torque density can be obtained in terms of only magnetic field using (10),

$$\boldsymbol{\tau}_v = \mu_0^{-1}\mathbf{r} \times ((\nabla \times \mathbf{B}) \times \mathbf{B}) \tag{14}$$

The concept of torque density does not provide any valuable information by its own. The sole purpose for this definition will be for only obtaining the net torque. It is also possible to define the surface torque density; however, as will be shown in the next section, the volume torque density suffices for obtaining the net torque.

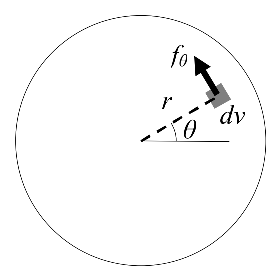

Fig. 4. Definition of the axial component of torque density using force density in cylindrical coordinates: $\tau_z = rf_\theta$.

Applicability of the Force Density Formulae

A magnetic body contains atomic currents. When magnetized, the miscancellation of these microscopic currents produce resultant macroscopic *bound currents*. The bound currents are in the form of

- a *magnetization surface current density* distribution at the surface of the body
- a *magnetization volume current density* distribution at its interior.

Relation (6) can be imposed where there exists a surface current density. Therefore, (6) applies to both

- the surface of a magnetic body or
- a current sheet with free current.

Relations (10), (11), and (14) can be imposed where there exists a volume current density. Therefore, these relations apply to both

- the volume of a magnetic body or
- a free bulk current.

Moreover, relations (6), (10), (11), and (14) are in terms of only the magnetic field, which provide an insight of the relation of force with magnetic field. The following conclusion is drawn:

- *A magnetic surface force density is generated when the magnetic field undergoes sudden changes in the form of spatial jump discontinuities.*
- *A magnetic volume force density is generated when the magnetic field undergoes smooth spatial variations, whether in magnitude or direction.*

3. Virtual Stresses

It is possible to rewrite the aforementioned electromagnetic force density as the derivative of new quantities. These new quantities – as will be shown – have physical interpretation and are analogous to mechanical *stress* and *traction*. However, these new quantities are not truly stress, therefore as the title of this section suggests, they should be rather called virtual stresses. In this section, the virtual stresses and their applications are introduced.

Maxwell Stress Tensor

Expression (10) provides a relation for computing the volume force density. At this point, current density is eliminated and the force density is obtained only in terms of magnetic field. However, a further simplification is possible. To this end, another one of the Maxwell equations is involved,

$$\nabla \cdot \mathbf{B} = 0 \tag{15}$$

Equation (15) is anonymous [15], however, it can be called Gauss's law for magnetism as an analogue of Gauss's law in electricity.

Knowing the fact that $(\nabla\cdot\mathbf{B})\mathbf{B} = 0$, the addition of this term with (10) does not alter it,

$$\mathbf{f}_v = \mu_0^{-1}\big((\nabla\times\mathbf{B})\times\mathbf{B} + (\nabla\cdot\mathbf{B})\mathbf{B}\big) \tag{16}$$

The above relation can be expressed in the form of the divergence of a tensor field $\boldsymbol{\sigma}$,

$$\mathbf{f}_v = \nabla\cdot\boldsymbol{\sigma} \tag{17}$$

In rectangular coordinates system, the *Maxwell stress tensor* $\boldsymbol{\sigma}$ is shown to be as follows (proof in Appendix 2-Theorem (4)),

$$\boldsymbol{\sigma} = \begin{bmatrix} \boldsymbol{\sigma}_x^{\,T} \\ \boldsymbol{\sigma}_y^{\,T} \\ \boldsymbol{\sigma}_z^{\,T} \end{bmatrix} = \begin{bmatrix} \sigma_{xx} & \sigma_{xy} & \sigma_{xz} \\ \hdashline \sigma_{yx} & \sigma_{yy} & \sigma_{yz} \\ \hdashline \sigma_{zx} & \sigma_{zy} & \sigma_{zz} \end{bmatrix} \tag{18}$$

where the components are,

$$\sigma_{ij} = \mu_0^{-1}\left(B_iB_j - \frac{1}{2}|\mathbf{B}|^2\delta_{ij}\right) \tag{19}$$

in which i and j denote the rectangular coordinate components x, y and z.

The tensor field is a collection of three vector fields: each row notated by $\boldsymbol{\sigma}_x$, $\boldsymbol{\sigma}_y$ and $\boldsymbol{\sigma}_z$. These vectors are distinguished by dashed lines in (18). Therefore, specifically, the tensor in here is a 3×3 matrix. The Kronecker delta δ is thereby a 3×3 identity matrix. The components of the tensor can be viewed as the elements of a matrix and the matrix algebra applies here. For instance, the inner product for the tensor is just like matrix multiplication.

Remark: The contribution of the electrostatic field and displacement current in the Maxwell stress tensor is not considered in this paper, because only the magnetic component is of interest. For a complete derivation of the Maxwell stress tensor, readers are referred to [15].

Physical Interpretation of Maxwell Stress Tensor

The Maxwell stress tensor, represented in (18), has a physical interpretation. An inference is derived from Equation (17): that the integral of $\boldsymbol{\sigma}$ over an infinitesimal *closed* surface is the volume force density. It means that $\boldsymbol{\sigma}$ has a physical dimension of force per area. This evidence will be encountered later in (36) as well. However, $\boldsymbol{\sigma}$ is a tensor as opposed to force which is a vector.

Although $\boldsymbol{\sigma}$ has an electromagnetic essence, equation (17) is indeed exactly in the form of the *equilibrium equation* in continuum mechanics [27],

$$\nabla\cdot\boldsymbol{\sigma}_m = -\mathbf{f} \tag{20}$$

where $\boldsymbol{\sigma}_m$ is the true mechanical stress tensor, also known as Cauchy stress tensor, and $\mathbf{f}$ is the external volume force density, also known as load or body force. Therefore, Maxwell stress tensor can borrow the concepts of mechanics. In that, the element σ_{ji} of stress tensor (19) is the force in direction i on the differential area oriented in the direction of j (Fig. 5). For instance, σ_{yx} is the force density in the direction of x acting on the differential surface $dxdz$, i.e. the surface with normal direction along y-

axis. The diagonal elements are normal stresses while the off-diagonal elements are shear stresses.

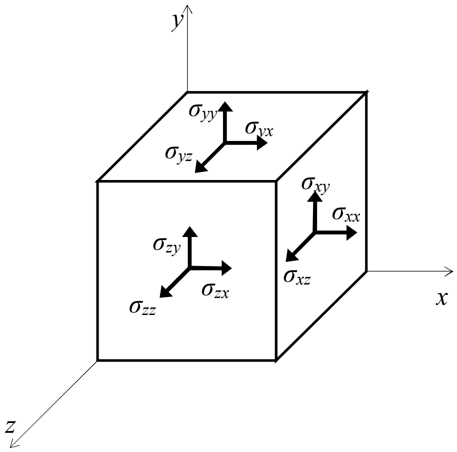

Fig. 5. Physical interpretation of Maxwell stress tensor components on the faces of a differential element in rectangular coordinates system. This interpretation is analogous to the mechanical stress tensor.

The above interpretation reveals why the name *stress* is used for Maxwell stress tensor. Although a physical insight was gained for it, Maxwell stress tensor $\boldsymbol{\sigma}$, is distinct from the true mechanical stress tensor $\boldsymbol{\sigma}_m$. The reason is that equation (17) merely states that the integral of $\boldsymbol{\sigma}$ over an infinitesimal *closed* surface is the volume force density. It does not give any information about an *open* surface (the 6 faces of the cube in Fig. 5). Therefore, localization of Maxwell stress tensor is incorrect [14].

Technically, stress is something that matter produces internally, as a mechanical response to external forces. From a mechanical perspective, even the equilibrium equation, i.e. (20), is not sufficient to obtain stress $\boldsymbol{\sigma}_m$ from external force density $\mathbf{f}$. The reason is that $\boldsymbol{\sigma}_m$ is a tensor with 9 components (to be specific, 6 unique components because of the symmetry) whereas $\mathbf{f}$ is a vector with only 3 components. Therefore only by the knowledge of $\mathbf{f}$, a unique $\boldsymbol{\sigma}$ cannot be found and more information is required to compute stress from external force. The additional information is in the context of elasticity which is beyond the scope of this paper. However, a few considerations are briefly noted in Section 7.

It was stated that the knowledge of force density distribution $\mathbf{f}$ is not sufficient information for deriving stress. However, the work of Maxwell has led to expressing the force distribution in terms of the divergence of a tensor field, only by means of the knowledge of force distribution! Indeed, the mathematical form of the electromagnetic force distribution has allowed such derivation. Although the mathematical work is elegant, Maxwell tensor is not truly the mechanical stress; because electromagnetic forces are exerted from an external source as stated earlier. There are other reasons that negate the Maxwell tensor from being the true stress tensor, e.g.

- Magnetic force exists only where there is current (whether applied or magnetization currents). However, Maxwell stress tensor gives a stress tensor field for any point in the space where magnetic field is present, even in vacuum. This clearly does not make sense as stress is only defined for matter (only magnetic materials in here).
- As mentioned before, a magnetic surface force density has a finite value only for a surface current density and is zero where a volume current density is present. This justifies that stress and traction exist only at the surface of a magnetic body. Because the surface magnetization currents are at the surface. However, Maxwell stress tensor can give a stress in the interior points as well.

The question is now, if Maxwell tensor is not stress, then what is it? The answer would become a matter of sophisticated dispute in a multidisciplinary context of physics and mathematics. It is now necessary to shorten the debate and to draw a conclusion. All that is certain is that in the context of continuum mechanics, the computation of stress requires both the external force density and the elastic properties of material.

Nevertheless, the Maxwell stress tensor is vastly accepted and frequently employed in the literature and even confirmed by experimental data [14].

More details on mechanical considerations are given in Section 7.

Maxwell Stress Vector

The surface force density over a specific plane can be viewed as the orientation of stress tensor along that plane. It is thus commonly known as *surface traction vector* or *stress vector* in mechanical engineering community. The traction $\mathbf{f}_s$ over an arbitrarily oriented surface with unit normal vector $\mathbf{a}_n$ has the following relation with stress tensor $\boldsymbol{\sigma}$.

$$\mathbf{f}_s = \boldsymbol{\sigma} \cdot \mathbf{a}_n \tag{21}$$

the *j*-th element of the traction vector $\mathbf{f}_s$ is obtained as

$$f_{s,i} = \left(\boldsymbol{\sigma} \cdot \mathbf{a}_n\right)_i = \sum_j \sigma_{ij} a_{n,j} \tag{22}$$

where $\mathbf{a}_{n,i}$ is the *i*-th element of the vector $\mathbf{a}_n$. Substituting (19) in (22),

$$f_{s,i} = \sum_j \sigma_{ij} a_{n,j} = \mu_0^{-1} \sum_j \left(B_i B_j - \frac{1}{2} |\mathbf{B}|^2 \delta_{ij} \right) a_{n,j}$$

$$f_{s,i} = \mu_0^{-1} \left(B_i \sum_j B_j a_{n,j} - \frac{1}{2} |\mathbf{B}|^2 \sum_j \delta_{ij} a_{n,j} \right)$$

$$f_{s,i} = \left(\boldsymbol{\sigma} \cdot \mathbf{a}_n\right)_i = \mu_0^{-1} \left(B_i \left(\mathbf{B} \cdot \mathbf{a}_n\right) - \frac{1}{2} |\mathbf{B}|^2 a_{n,i} \right) \tag{23}$$

Relation (23) provides a straightforward approach to compute the traction vector in the global coordinate system (*x*,*y*,*z*). It is noted that this relation is valid for any surface, since $\mathbf{a}_n$ is chosen arbitrarily. The relation also holds at any point whether interior or at the surface of the magnetic body of interest.

It will be more interesting to restate the traction in a local coordinate system. Let us consider a local two-dimensional coordinate system (t,n) at an arbitrary plane on which traction is to be determined. t and n are respectively the tangent and normal directions on the considered plane. Since a plane has a unique normal direction and an infinite number of tangent directions, n is unique whilst an infinite number of choices exist for t. By substituting $i=\{t,n\}$ in (23) one obtains the simple formula of

$$\begin{cases} f_{s,t} = \mu_0^{-1} B_t B_n \\ f_{s,n} = \mu_0^{-1}\left(B_n^{\,2} - \frac{1}{2}|\mathbf{B}|^2\right) \end{cases} \tag{24}$$

where a few hints are noted:

- $\mathbf{a}_{n,t} = \mathbf{a}_n \cdot \mathbf{a}_t = 0$
- $\mathbf{a}_{n,n} = \mathbf{a}_n \cdot \mathbf{a}_n = 1$
- $B_n = \mathbf{B} \cdot \mathbf{a}_n$

The normal component of traction $f_{s,n}$ is known as the *normal* (*tensile*/*compressive*) stress and the tangent component $f_{s,t}$ is called the *shear* stress on a particular surface. The normal stress is sometimes interchanged with *pressure* [15]; however, pressure refers to external forces.

Relation (24) provides an easy method of computing the stress at a surface where the normal and tangent components of the magnetic field are known.

It might be inferred that relation (24) holds for only 2-D space. Reference [14] has indeed obtained it for the special case of 2-D space. However, in here it was shown that the relation is valid for 3-D space, because the tangent direction is arbitrary. For example, if one chooses the z-axis as the normal axis $n=z$, then the tangent axes would be the two others $t=\{x,y\}$.

Relation (24) has been used by many authors to compute the traction force at the surface of the stator/rotor of electrical machines under the name of local tractions e.g. [10]. However, as mentioned before, the localization of the Maxwell stress tensor is incorrect for the computation of surface force density [14]. Since the correct formula of surface force density is already derived in Section 2, a comparison is now possible. The Maxwell stress vector, i.e. (24), is somewhat comparable with the formula (8);

$$\begin{cases} f_{s,t} = -\mu_0^{-1} B_{FM,t} B_n \\ f_{s,n} = \frac{1}{2}\mu_0^{-1} B_{FM,t}^{\;\;2} \end{cases}$$

As is evident, the tangent components of surface force density in both formulas are identical (ignoring the sign), whereas the normal components still have a discrepancy. The conclusion is: *The Maxwell stress vector represented in (24) is only valid for the tangent component of surface force density at the surface of a perfect ferromagnetic material with no free surface current.*

Actual Stress Vector

It was stated that the Maxwell stress vector represented in (24) is not the true stress vector (surface traction). At the end of Section 2, a conclusion was drawn that a surface force density exists at a surface of flux discontinuity. Therefore, it is instructive to study the Maxwell stress tensor in such a condition.

As a consequence of the discontinuity in flux density, the Maxwell stress tensor will be discontinuous. As a result, the derivative in (17) is no longer possible. Instead, the boundary condition must be investigated. Assume a differential box with volume $dv=(dh)(ds)$ on the considered surface. The box is wafer-shaped with the thickness dh negligible compared to ds (Fig. 6).

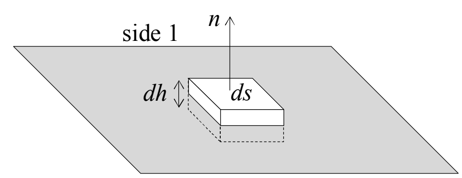

Fig. 6. A thin wafer-shaped box at some interface of discontinuous magnetic flux.

According to (36), the force exerted to dv is approximately

$$d\mathbf{F} = \oint_S \boldsymbol{\sigma} \cdot \mathbf{ds} \approx (\boldsymbol{\sigma}_1 - \boldsymbol{\sigma}_2) \cdot \mathbf{a}_n ds$$

where $\mathbf{a}_n$ is the unit normal vector pointing from side "2" to side "1" of the surface. The integral over the lateral area is neglected because dh is negligible compared to ds. Therefore, the surface force density will be as follows

$$\mathbf{f}_s = (\boldsymbol{\sigma}_1 - \boldsymbol{\sigma}_2) \cdot \mathbf{a}_n \tag{25}$$

Substituting (19) in (25) using the notation of (22), to give the i-th component of $\mathbf{f}_s$,

$$f_{s,i} = ((\boldsymbol{\sigma}_1 - \boldsymbol{\sigma}_2) \cdot \mathbf{a}_n)_i = \sum_j (\sigma_{ij,1} - \sigma_{ij,2}) a_{n,j}$$

$$f_{s,i} = \mu_0^{-1} \sum_j \begin{pmatrix} +\left(B_{i1}B_{j1} - \frac{\delta_{ij}}{2}|\mathbf{B}_1|^2\right) \\ -\left(B_{i2}B_{j2} - \frac{\delta_{ij}}{2}|\mathbf{B}_2|^2\right) \end{pmatrix} a_{n,j}$$

$$f_{s,i} = \mu_0^{-1} \begin{pmatrix} +\left(B_{i1}(\mathbf{B}_1 \cdot \mathbf{a}_n) - \frac{1}{2}|\mathbf{B}_1|^2 a_{n,i}\right) \\ -\left(B_{i2}(\mathbf{B}_2 \cdot \mathbf{a}_n) - \frac{1}{2}|\mathbf{B}_2|^2 a_{n,i}\right) \end{pmatrix}$$

using the continuity of normal flux density, the following simple formula is obtained

$$f_{s,i} = \mu_0^{-1}\left((B_{i1} - B_{i2})B_n - \frac{1}{2}\left(|\mathbf{B}_1|^2 - |\mathbf{B}_2|^2\right)a_{n,i} \right) \quad (26)$$

In the special case of 2-D field distribution, by defining a local (t-n) frame, $i=\{t,n\}$ can be substituted in (26),

$$\begin{cases} f_{s,t} = \mu_0^{-1}(B_{t1} - B_{t2})B_n \\ f_{s,n} = -\mu_0^{-1}\frac{1}{2}\left(B_{t1}^{\ 2} - B_{t2}^{\ 2}\right) \end{cases} \quad (27)$$

The above relation matches (7). Relation (27) shows that: *In contrast with the Maxwell stress vector represented in (24), the boundary condition of the Maxwell stress tensor given in (27) accounts for the actual stress vector.*

Maxwell Couple Stress Tensor

It was shown that force density (10) can be rewritten as the divergence of a tensor called the *Maxwell stress tensor*. Additionally, torque density (14) can be expressed as the divergence of another tensor that is named henceforth *Maxwell couple stress tensor*.

$$\boldsymbol{\tau}_v = \nabla \cdot \mathbf{m} \quad (28)$$

It was shown that the name Maxwell stress tensor is borrowed from mechanical concepts but it does not exactly reflect the name. The concept of Maxwell couple stress tensor also follows the same rule and therefore, the authors of this paper adopted this name. More details are given in the subsection entitled “Physical Interpretation of Maxwell Couple Stress Tensor”.

Maxwell couple stress tensor $\mathbf{m}$ in rectangular coordinates is shown to be as follows (Appendix 2-Theorem (8))

$$\mathbf{m} = \begin{bmatrix} \mathbf{m}_x^{\ T} \\ \mathbf{m}_y^{\ T} \\ \mathbf{m}_z^{\ T} \end{bmatrix} = \begin{bmatrix} m_{xx} & m_{xy} & m_{xz} \\ \hdashline m_{yx} & m_{yy} & m_{yz} \\ \hdashline m_{zx} & m_{zy} & m_{zz} \end{bmatrix} \quad (29)$$

the components can be expressed in terms of the components of the Maxwell stress tensor $\boldsymbol{\sigma}$ and the location vector $\mathbf{r}$,

$$m_{ij} = \left(\mathbf{r} \times \boldsymbol{\sigma}_j\right)_i \quad (30)$$

in which i and j denote the rectangular coordinate components x, y and z.

Similarly, each row of $\mathbf{m}$, notated by $\mathbf{m}_x$, $\mathbf{m}_y$ and $\mathbf{m}_z$, is a vector field and is distinguished by dashed lines in the tensor (29).

Equivalently, $\mathbf{m}$ can be denoted by

$$\mathbf{m} = \left(\mathbf{r} \times \mathbf{T}\right)^T \quad (31)$$

where superscript T is the notation of transpose.

Couple Stress Vector

Previously, a generic tensor field $\mathbf{m}$ was found in rectangular coordinates which divergence equals the volume torque density vector $\boldsymbol{\tau}$. However in many applications, the torque needs to be found only along a specific axis; for convenience, the z-axis. One exemplary application is for electrical machines.

Here, a straightforward formula is proposed for the z-component of Maxwell couple stress tensor $\mathbf{m}_z$ that is used for obtaining the z-component of the torque. This imposes no loss of generality, as the orientation of the local coordinates is arbitrary.

The attempt is to obtain the vector $\mathbf{m}_z$ in cylindrical coordinates. In this case, (28) simplifies to

$$\tau_z = r f_\theta = \nabla \cdot \mathbf{m}_z \quad (32)$$

In this simple case, τ_z, the axial component of volume torque density vector ($\boldsymbol{\tau}$) is equal to the multiplication of r, the radial component of the location vector ($\mathbf{r}$) and f_θ, the tangential component of volume force density ($\mathbf{f}$).

In the cylindrical coordinate system, the *Couple Stress Vector* $\mathbf{m}_z$ is derived as (Appendix 2-Theorem (6)),

$$\mathbf{m}_z = \begin{bmatrix} m_{zr} \\ m_{z\theta} \\ m_{zz} \end{bmatrix} \quad (33)$$

where the components are,

$$m_{zi} = \mu_0^{-1} r\left(B_i B_\theta - \frac{1}{2}|\mathbf{B}|^2 \delta_{i\theta} \right) \quad (34)$$

in which δ is the Kronecker delta and i denotes the cylindrical coordinate components r, θ and z.

The formula (34) is very concise and compactly expressed in terms of the magnetic field as opposed to (30) and looks very much like (19), however, in cylindrical coordinates. In case $\mathbf{m}_x$ or $\mathbf{m}_y$ are to be found, the coordinate system can be oriented such that the new z-axis aligns with the old x-axis or the y-axis.

Important Note

in the expression (34),

- The variable r is a part of $\mathbf{m}_z$ and undergoes differentiation when computing $\nabla\cdot\mathbf{m}_z$, thus cannot be moved outside of the divergence. That is, it is not correct to deduce that,

$$r f_\theta = \nabla \cdot \mu_0^{-1} r \begin{bmatrix} B_r B_\theta \\ B_\theta^{\ 2} - \frac{1}{2}|\mathbf{B}|^2 \\ B_z B_\theta \end{bmatrix} \rightarrow f_\theta = \nabla \cdot \mu_0^{-1} \begin{bmatrix} B_r B_\theta \\ B_\theta^{\ 2} - \frac{1}{2}|\mathbf{B}|^2 \\ B_z B_\theta \end{bmatrix}$$

- The vector term without r under the action of divergence ($\mathbf{m}/r$) is exactly in the form of the second row of Maxwell stress tensor in rectangular coordinates, however, with (r,θ,z) subscripts instead of (x,y,z). This is a COINCIDENCE and it is not logical to deduce that the Maxwell stress tensor assumes the same form in cylindrical coordinates as it does in rectangular coordinates. This statement is proved in Appendix 2-Theorem (5).

Physical Interpretation of Maxwell Couple Stress Tensor

The main difference of the Maxwell couple stress tensor with the Maxwell stress tensor is that in contrast with Maxwell stress tensor, the Maxwell couple stress tensor resembles the rotational force. However, in view of physical interpretation, the Maxwell couple stress tensor is analogous to Maxwell stress tensor in every aspect. Therefore the interpretations of Maxwell stress tensor can be converted appropriately to describe the Maxwell couple stress tensor.

The equation of (32) is exactly in the form of the rotational (angular or momentum) equilibrium equation in mechanics. It is thus the rotational analogue of the equilibrium equation (20).

From (28), it is evident that the physical dimension of the Maxwell couple stress tensor is torque per unit area, whereas the physical dimension of the Maxwell stress tensor is force per unit area.

The component m_{ij} of the Maxwell couple stress tensor can be interpreted as the torque generated by the stress components acting on the j-plane (the plane with a normal vector in the j-direction) about the i-axis. For instance, m_{xy} represents the torque due to the stress components located on the xz-plane (i.e., the surface perpendicular to the y-direction) about the x-axis.

The abovementioned physical interpretations, although they seem satisfying, are abstract. because the basis of inference is similar to that of the Maxwell stress tensor. Therefore, once again, the rotational analogue of the concept of stress and traction is dependent upon the mechanical response of the material.

The concept of Maxwell couple stress tensor is extended from Maxwell stress tensor to consider the rotational effect. This concept is the work of the authors of this paper. The authors have adopted the name *Maxwell couple stress tensor* for the tensor field **m** to resemble the rotational effect.

4. Resultant (Net) Force

There are two types of rigid motion (assuming no deformation), which are both practical in electrical machines.

- Linear (translational) motion
- Rotating (angular) motion

These motions are due to the existence of respectively a nonzero resultant force and a net torque exerted on a body.

To obtain the total magnetic force exerted on a magnetic body, two principal physical laws can be employed.

- Lorentz force law
- Principle of conservation of energy

In this section, the Lorentz force law is investigated and the energy method is separately discussed in the next section.

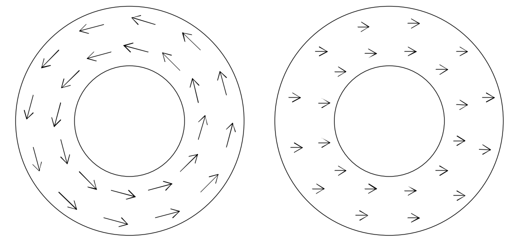

Fig. 7. Visualizing the tangential component (left) and the horizontal component (right) of elemental force vectors **dF** in an exemplary body (e.g., rotor of an electrical machine). These forces result in rotational and translational motions.

Resultant Force

The resultant force **F** is the sum of all elemental forces $d\mathbf{F}$ over the volume V of the body under study (Fig. 7).

$$\mathbf{F} = \int_V d\mathbf{F}$$

By aid of the concept of volume force density (3), the above can be restated as

$$\mathbf{F} = \int_V \mathbf{f}_v dv \tag{35}$$

and in terms of the Maxwell stress tensor (17),

$$\mathbf{F} = \int_V \nabla \cdot \boldsymbol{\sigma} dv$$

Now, the application of the divergence theorem reduces the volume integral to a surface integral,

$$\mathbf{F} = \oint_S \boldsymbol{\sigma} \cdot d\mathbf{s} \tag{36}$$

Relation (36) yields the resultant force exerted on the magnetic system bounded by the surface S. It is noted that each component of the resultant force F_i corresponds to the integral of the corresponding vector (each row) of the Maxwell stress tensor $\boldsymbol{\sigma}_i$.

$$\begin{cases} F_x = \int_S \boldsymbol{\sigma}_x \cdot d\mathbf{s} \\ F_y = \int_S \boldsymbol{\sigma}_y \cdot d\mathbf{s} \\ F_z = \int_S \boldsymbol{\sigma}_z \cdot d\mathbf{s} \end{cases}$$

Net Torque

The net torque τ is the sum of all elemental torques across the volume V of a body (Fig. 7).

$$\mathbf{T} = \int_V d\mathbf{T}$$

Using the concept of torque density $\boldsymbol{\tau}$ (13), the net torque can be restated as

$$\mathbf{T} = \int_V \boldsymbol{\tau} dv \tag{37}$$

In terms of the couple stress vector (32), the above would become

$$\mathbf{T} = \int_V \nabla \cdot \mathbf{m} dv$$

and with the application of divergence theorem,

$$\mathbf{T} = \oint_S \mathbf{m} \cdot d\mathbf{s} \tag{38}$$

Relation (38) is capable of obtaining the net torque exerted to the entire magnetic system contained within the closed surface S. This relation is analogous with (36).

Remark: The net torque **T** obtained from (28) is given in (38) as a generic formula. If only the z-component is considered, i.e. as in (32), then (38) reduces to

$$T_z = \oint_S \mathbf{m}_z \cdot d\mathbf{s}$$

Remark: If the body is surrounded by vacuum or any non-magnetic material without current, S can be extended to a larger surface in (36) and (38); because the electromagnetic force to the additional surrounding space is null.

5. Energy Method

In this section, the total magnetic force and magnetic torque are derived using the principle of conservation of energy.

According to this physical law, the total amount of energy is conserved, but it can change form. In this approach, force can be calculated using either the magnetic energy or the co-energy, which both lead to identical results.

Calculation of Force Using Energy/Co-energy

For an electro-magneto-mechanical system, the magnetic energy can be obtained via the energy balance equation [18], [19] and the co-energy is defined in terms of it as follows,

$$\begin{aligned} dW_{\text{mag}} &= dW_{\text{elec}} - dW_{\text{mech}} \\ dW'_{\text{mag}} &= d(i\lambda) - dW_{\text{mag}} \end{aligned} \tag{39}$$

where dW_{mag}, dW_{elec}, dW_{mech} are respectively the differential change of magnetic, electric and mechanical energy transferred in and out of the system and i and λ are the current and flux linkage of the current-carrying elements.

Knowing that $dW_{\text{elec}}=i(d\lambda/dt)dt$, where Faraday's induction law was used, and that the mechanical work is the product of force by displacement, (39) can be rewritten as,

$$\begin{aligned} dW_{\text{mag}} &= i d\lambda - \begin{cases} \mathbf{F} \cdot d\mathbf{x} & \text{linear motion} \\ T_z d\theta_r & \text{rotary motion} \end{cases} \\ dW'_{\text{mag}} &= \lambda di + \begin{cases} \mathbf{F} \cdot d\mathbf{x} & \text{linear motion} \\ T_z d\theta_r & \text{rotary motion} \end{cases} \end{aligned} \tag{40}$$

in which $\mathbf{dx}$ and $d\theta_r$ are the differential translational and rotational displacements of either a movable or a stationary part. For computation of force of the stationary parts, the displacement is virtual rather than actual; hence the method is also known as *virtual displacement* or *virtual work* method.

Equations (40) show that the magnetic energy can vary with flux linkage and displacement and the magnetic co-energy can vary with current and displacement. Therefore each of the energy/co-energy is a function of their respective variables. The differential change of energy/co-energy can be written as their partial derivatives with respect to their variables,

$$\begin{cases} dW_{\text{mag}}(\lambda,\mathbf{x}) = \dfrac{\partial W_{\text{mag}}}{\partial \lambda} d\lambda + \dfrac{\partial W_{\text{mag}}}{\partial \mathbf{x}} \cdot d\mathbf{x} & \\ dW'_{\text{mag}}(i,\mathbf{x}) = \dfrac{\partial W'_{\text{mag}}}{\partial i} di + \dfrac{\partial W'_{\text{mag}}}{\partial \mathbf{x}} \cdot d\mathbf{x} & \text{linear motion} \\ \hline dW_{\text{mag}}(\lambda,\theta_r) = \dfrac{\partial W_{\text{mag}}}{\partial \lambda} d\lambda + \dfrac{\partial W_{\text{mag}}}{\partial \theta_r} d\theta_r & \\ dW'_{\text{mag}}(i,\theta_r) = \dfrac{\partial W'_{\text{mag}}}{\partial i} di + \dfrac{\partial W'_{\text{mag}}}{\partial \theta_r} d\theta_r & \text{rotary motion} \end{cases} \tag{41}$$

A comparison of (41) and (40) yields,

$$\begin{cases} \mathbf{F} = -\nabla W_{\text{mag}}(\lambda,\mathbf{x})\big|_{\lambda} = \nabla W'_{\text{mag}}(i,\mathbf{x})\big|_{i} & \text{linear motion} \\ T_z = -\dfrac{\partial W_{\text{mag}}(\lambda,\theta_r)}{\partial \theta_r}\bigg|_{\lambda} = \dfrac{\partial W'_{\text{mag}}(i,\theta_r)}{\partial \theta_r}\bigg|_{i} & \text{rotary motion} \end{cases} \tag{42}$$

where ∇ is the differentiation with respect to the displacement vector $\mathbf{x}$.

In (42), the spatial partial derivatives of W_{mag} and W'_{mag} must be performed in the condition of λ=constant and i=constant, respectively, because the partial derivative of a multivariate function with respect to a certain variable is conducted such that the remaining variables are held constant.

Calculation of Energy/Co-energy

It was shown how the force can be calculated from magnetic energy/co-energy (42); however, the calculation of these quantities must be discussed separately. To this end, W_{mag} and W'_{mag} can be calculated by integrating their differential values (40), but since the functions are bivariate, the integrations can be performed on an infinite number of integration paths. Knowing that the functions only depend on the steady-state values of their respective variables, the integrals are not path-dependent. The simplest integration path is as follows: while $\{\mathbf{x},\theta_r\}$=constant, λ for W_{mag} and i for W'_{mag} are increased to their respective steady-state values,

$$\begin{cases} W_{\text{mag}} = \displaystyle\int_{\lambda=0}^{\lambda=\lambda_{ss}} i d\lambda \\ W'_{\text{mag}} = \displaystyle\int_{i=0}^{i=i_{ss}} \lambda di \end{cases} \tag{43}$$

where the subscript "ss" denotes steady-state.

Since λ is unknown, it is better to express the above relations in terms of magnetic field. If the current-carrying elements are imagined as an aggregation of filaments with infinitesimal cross-sections, then (43) can be rewritten as:

$$\begin{cases} W_{\text{mag}} = \int_T \int_S di\, d\phi \\ W'_{\text{mag}} = \int_T \int_S \phi d(di) \end{cases} \tag{44}$$

where

- di is the current of the consisting filaments having the contour path of C and cross-section ds,
- $d(di)$ is the temporal differential change of di,
- $d\varphi$ is the temporal differential change of magnetic flux of the filaments,
- S is the total surface of the current carrying elements and
- T is the total time from beginning to steady-state.

The magnetic flux can be obtained using line integration of magnetic vector potential **A** along filament C as follows,

$$\phi = \oint_C \mathbf{A} \cdot d\mathbf{l}$$

where $d\mathbf{l}$ is the differential length element of C.

Substituting the above relation in (44) yields,

$$\begin{cases} W_{\text{mag}} = \int_T \int_S di \oint_C d\mathbf{A} \cdot d\mathbf{l} = \int_T \int_S \oint_C d\mathbf{A} \cdot (di d\mathbf{l}) \\ W'_{\text{mag}} = \int_T \int_S d(di) \oint_C \mathbf{A} \cdot d\mathbf{l} = \int_T \int_S \oint_C \mathbf{A} \cdot d(di d\mathbf{l}) \end{cases} \tag{45}$$

It is noted that in the second integral, $d(di)d\mathbf{l}=d(did\mathbf{l})$, because the outer d denotes temporal differentiation while the inner d is for spatial differentiation. Now using the fact that,

$$did\mathbf{l} = \frac{di}{ds}\mathbf{a}_t (dsdl) = \mathbf{J}dv$$

in which, $\mathbf{a}_t$ is the unit tangent vector of filaments, **J** is the volume current density and dv is the volume element, (45) can be obtained as follows,

$$\begin{cases} W_{\text{mag}} = \int_T \int_V d\mathbf{A} \cdot \mathbf{J} dv \\ W'_{\text{mag}} = \int_T \int_V \mathbf{A} \cdot d\mathbf{J} dv \end{cases} \tag{46}$$

in which $d\mathbf{A}$ and $d\mathbf{J}$ denote the temporal differential change of the respective quantities.

It is notable that **J** only denotes the applied or free currents of the system and not the magnetization currents, because this formulation is derived from i, the currents in the coils. If the system includes permanent magnets, the remanent flux density $\mathbf{B}_{rem}$ also acts as applied current with the following relation,

$$\begin{cases} \mu_0 \mathbf{J}_{m,rem,v} = \nabla \times \mathbf{B}_{rem} \\ \mu_0 \mathbf{J}_{m,rem,s} = \mathbf{B}_{rem} \times \mathbf{a}_n \end{cases} \tag{47}$$

where $\mathbf{J}_{m,rem,v}$ and $\mathbf{J}_{m,rem,s}$ are the volume and surface magnetization current densities of the permanent magnets and $\mathbf{a}_n$ is the unit normal vector at their surface.

In many references, (46) is rewritten in terms of **B** and **H** and the reason is that it is conventional to only work with field quantities [13]. This formulation is suitable for FEM where it is needed to minimize the energy functional [20]. Formulation in terms of **B** and **H** will result in a volume integral in the entire space. However in analytical models, working with **A** and **J** requires less computational effort; because volume integral is only performed on the windings or permanent magnets. Also since **B** is the derivative of **A**; **A** is smoother than **B** and **H** and therefore, no loss of accuracy due to differentiation arise.

Reyne Stress Tensor

There has been a dispute over a unique definition of local magnetic forces. An extensive research illuminates several mismatching results for a handful of methods [16]. As was mentioned in Section 2, the Maxwell stress tensor cannot be localized to obtain surface tractions. Therefore there is a need to resort to energy method. A modification of Maxwell stress tensor has been carried out by Reyne based on energy conservation. The resulting stress tensor is referred to as *nonlinear Maxwell stress tensor* [17] or as the name of the proposer, *Reyne stress tensor* [14]. This method is suitable for finite element analysis. It has been used to predict vibration.

6. APPLICATION IN ROTATING MACHINES

In this section, the generic formulae derived earlier are simplified in the case of rotating electrical machines.

In many machine modeling cases, it is conventional to set a few assumptions for the sake of model simplification. In this section, some applicable simplified expressions using the aforementioned approaches are derived for the case of 2-D rotary structures.

Surface Traction (*Stress Vector*)

In a rotating electrical machine, the surface force density is most forceful at the surface of stator/rotor teeth which face the air gap. Therefore, it is required to compute the radial and azimuthal components of surface force density on the curved faces of the teeth. For an inner-rotor rotating motor, the force density at the surface of stator teeth can be obtained by substituting 1=stator, 2=air-gap, $n = r$ and $t = -\theta$ in (7),

$$\begin{cases} f_{s,t} = \mu_0^{-1}(B_{1,t} - B_{2,t})B_n \\ f_{s,n} = -\frac{1}{2}\mu_0^{-1}(B_{1,t}^{\ 2} - B_{2,t}^{\ 2}) \end{cases}$$

$$\begin{cases} -f_{s,\theta} = \mu_0^{-1}(-B_{\text{stator},\theta} - (-B_{\text{gap},\theta}))B_r \\ f_{s,r} = -\frac{1}{2}\mu_0^{-1}((-B_{\text{stator},\theta})^2 - (-B_{\text{gap},\theta})^2) \end{cases}$$

to obtain,

$$\begin{cases} f_{s,\text{stator},\theta} = \mu_0^{-1}(B_{\text{stator},\theta} - B_{\text{gap},\theta})B_r \\ f_{s,\text{stator},r} = -\frac{1}{2}\mu_0^{-1}(B_{\text{stator},\theta}^{\ 2} - B_{\text{gap},\theta}^{\ 2}) \end{cases} \tag{48}$$

and of rotor teeth can be obtained by substituting 1=air-gap, 2=rotor, $n = r$ and $t = -\theta$ in (7),

$$\begin{cases} f_{s,t} = \mu_0^{-1}\left(B_{1,t} - B_{2,t}\right)B_n \\ f_{s,n} = -\frac{1}{2}\mu_0^{-1}\left(B_{1,t}^{\ 2} - B_{2,t}^{\ 2}\right) \end{cases}$$

$$\begin{cases} -f_{s,\theta} = \mu_0^{-1}\left(-B_{\text{gap},\theta} - \left(-B_{\text{rotor},\theta}\right)\right)B_r \\ f_{s,r} = -\frac{1}{2}\mu_0^{-1}\left(\left(-B_{\text{gap},\theta}\right)^2 - \left(-B_{\text{rotor},\theta}\right)^2\right) \end{cases}$$

to obtain,

$$\begin{cases} f_{s,\text{rotor},\theta} = \mu_0^{-1}\left(B_{\text{gap},\theta} - B_{\text{rotor},\theta}\right)B_r \\ f_{s,\text{rotor},r} = -\frac{1}{2}\mu_0^{-1}\left(B_{\text{gap},\theta}^{\ 2} - B_{\text{rotor},\theta}^{\ 2}\right) \end{cases} \quad (49)$$

In case no free surface current is present at the surface of the stator/rotor tooth and the magnetic reluctance of the tooth is neglected, $B_{\text{gap},\theta}=0$ can be presumed.

One can easily obtain the surface force density formula at the surface of slot walls in a similar approach. However, they are negligible.

Resultant Force Based on Lorentz Force

The magnetic field distribution can be assumed to be completely two-dimensional. In the case of radial flux rotary structures, 2-D field presumes that $B_z=0$. For the calculation of electromagnetic torque of the rotor, the couple stress vector (38) can be employed, where S can typically be a cylindrical surface in the air-gap surrounding the rotor. This choice has the advantage that for all surface elements, the radius of the adopted cylindrical surface in the air-gap is constant, $r=r_g$. Knowing that $d\mathbf{s}=L_z r_g d\theta \mathbf{a}_r$ in which L_z is the axial length, (38) is simplified as follows

$$T_z = \mu_0^{-1} L_z r_g^{\ 2} \int_0^{2\pi} B_r B_\theta d\theta \quad (50)$$

To account for the mechanical issues in the design of electrical machines, unbalanced forces should be computed as well. These forces include the ones that tend to displace the rotor from its balanced location; thus, the Maxwell stress tensor, either in the form of (96) or (99), can be employed. However, since the integration surface S is cylindrical-shaped, a cylindrical coordinate system is preferred, and thus (99) looks more appropriate. Substituting (99) in (36) using the aforementioned assumptions, the force can be simplified as follows:

$$\begin{cases} F_x = \mu_0^{-1} L r_g \int_0^{2\pi} \frac{1}{2}\cos(\theta)\left(B_r^{\ 2} - B_\theta^{\ 2}\right) - \sin(\theta) B_r B_\theta d\theta \\ F_y = \mu_0^{-1} L r_g \int_0^{2\pi} \frac{1}{2}\sin(\theta)\left(B_r^{\ 2} - B_\theta^{\ 2}\right) + \cos(\theta) B_r B_\theta d\theta \end{cases} \quad (51)$$

For the computation of electromagnetic or reluctance or cogging torques, (50), and for the computation of radial magnetic forces, (51) seem to be sufficiently compact and simple. However, it is worth to find even simpler expressions out of these formulas. Consider the following definition,

$$\begin{cases} B_\theta = |B|\sin(\phi) \\ B_r = |B|\cos(\phi) \end{cases} \rightarrow \begin{cases} |B|^2 = B_\theta^{\ 2} + B_r^{\ 2} \\ \tan(\phi) = B_\theta / B_r \end{cases} \quad (52)$$

where $|\mathbf{B}|$ is the magnitude of magnetic field and φ is the angle between $\mathbf{B}$ and the radial direction visualized in Fig. 8 and both depend on azimuth θ.

Substituting (52) in (50) and (51) results in the following

$$T_z = \mu_0^{-1} L_z r_g^{\ 2} \int_0^{2\pi} \frac{1}{2}|B|^2 \sin(2\phi) d\theta \quad (53)$$

$$\begin{cases} F_x = \mu_0^{-1} L_z r_g \int_0^{2\pi} \frac{1}{2}|B|^2 \cos(\theta + 2\phi) d\theta \\ F_y = \mu_0^{-1} L_z r_g \int_0^{2\pi} \frac{1}{2}|B|^2 \sin(\theta + 2\phi) d\theta \end{cases} \quad (54)$$

These relations look more insightful, because working with magnitude and direction is always more straightforward than the combination of coordinate components. Also using,

$$B_x = |B|\cos(\theta + \phi)$$

$$B_y = |B|\sin(\theta + \phi)$$

$$\cos(\theta + 2\phi) = \cos(\theta + \phi)\cos(\phi) - \sin(\theta + \phi)\sin(\phi)$$

$$\sin(\theta + 2\phi) = \sin(\theta + \phi)\cos(\phi) + \cos(\theta + \phi)\sin(\phi)$$

another equivalent expression can be derived

$$\begin{cases} F_x = \mu_0^{-1} L_z r_g \int_0^{2\pi} \frac{1}{2}\left(B_x B_r - B_y B_\theta\right) d\theta \\ F_y = \mu_0^{-1} L_z r_g \int_0^{2\pi} \frac{1}{2}\left(B_y B_r + B_x B_\theta\right) d\theta \end{cases} \quad (55)$$

Based on Conservation of Energy

For linear media, the λ-i characteristic is linear ($\lambda=Li$: L is the inductance coefficient) and (43) simplifies as follows,

$$W_{\text{mag}} = \frac{1}{2}\lambda_{ss} i_{ss} = W'_{\text{mag}} \quad (56)$$

Since the final state of magnetic energy/co-energy does not depend on how the current and flux linkage reach their steady-state, it is possible to assume that the applied current $\mathbf{J}$ increases linearly over time to its steady-state $\mathbf{J}_{ss}$. As a result of the linear magnetization characteristic, the magnetic field $\mathbf{A}$ will also have a linear characteristic over time, thus satisfying the following relations,

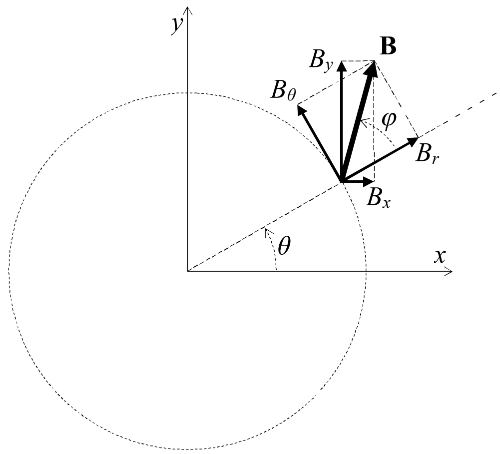

Fig. 8. Visualizing the angle φ used in expression (52). The circular dashed line indicates the integration line in air-gap for force computation.

$$\mathbf{A}(t) = \frac{t}{T}\mathbf{A}_{ss}$$

$$\mathbf{J}(t) = \frac{t}{T}\mathbf{J}_{ss}$$

Substituting in (46) yields,

$$W_{\text{mag}} = W'_{\text{mag}} = \frac{1}{2}\int_V \mathbf{A}_{ss}\cdot\mathbf{J}_{ss}dv \quad (57)$$

In the case of a 2-D field, both **A** and **J** have only z component,

$$W_{\text{mag}} = W'_{\text{mag}} = \frac{1}{2}\int_V A_z J_z dv \quad (58)$$

Where the "*ss*" subscript is not written for the convenience of notation.

Now the electromagnetic torque can be obtained by substituting (58) in (42).

$$\tau \cong \frac{1}{2}\frac{\Delta\int_V A_z J_z dv}{\Delta\theta_r}\Bigg|_J \quad (59)$$

In the above formula, the finite difference notation is used instead of the derivative; the reason is that it is often not possible to obtain the magnetic field in the form of an analytic function of rotor position. Thus, it is best to solve for the magnetic field at various discrete rotor positions. In addition, the electromagnetic torque is obtained under the condition of J=constant; because current is a known value of the problem, while λ is unknown, and thus keeping current constant is more straightforward.

Formulas Based on Harmonic Model

A conventional method to model the magnetic field of electrical machines is the SVM (also known as the sub-domain method, Fourier or harmonic model) in which the magnetic field distribution across azimuthal direction is in the form of trigonometric Fourier series [21].

$$A_z = \sum_{k=1}^{\infty} R[k](r)\Theta[k](\theta) \quad (60)$$

where the azimuthal eigenfunctions Θ and the eigenvalues λ are as follows,

$$\begin{cases}\Theta[2k-1](\theta) = \cos(\lambda[2k-1]\theta)/\sqrt{\pi} \\ \Theta[2k](\theta) = \sin(\lambda[2k]\theta)/\sqrt{\pi} \\ \lambda[2k-1] = \lambda[2k] = k \in \{1,2,3,\ldots\}\end{cases} \quad (61)$$

and $R[k](r)$ is the k-th coefficient of expansion at radius r. The eigenfunctions are orthonormal,

$$\int_0^{2\pi}\Theta[k](\theta)\Theta[n](\theta)d\theta = \delta[n,k] \quad (62)$$

in which δ is the Kronecker delta.

In two-dimensional field distribution, the magnetic flux density can be obtained from,

$$\begin{cases}B_r = \dfrac{1}{r}\dfrac{\partial A_z}{\partial\theta} \\ B_\theta = -\dfrac{\partial A_z}{\partial r}\end{cases} \quad (63)$$

Substituting (60) in (63),

$$\begin{cases}B_r = \sum_{k=1}^{\infty}\dfrac{1}{r}R[k](r)\Theta'[k](\theta) \\ B_\theta = \sum_{k=1}^{\infty} -R'[k](r)\Theta[k](\theta)\end{cases} \quad (64)$$

however, B_r is written in terms of the derivative of the eigenfunctions. To obtain the eigenfunction expansion, the following identity can be used,

$$\sum_{k=1}^{\infty} f[k]\Theta'[k](\theta) = \sum_{k=1}^{\infty}\lambda[k]\zeta(f[k])\Theta[k](\theta) \quad (65)$$

where f is an arbitrary sequence and operator ζ is defined as,

$$\zeta(f[n]) = \sum_{k=1}^{\infty} f[k]\frac{1}{\lambda[n]}\int_0^{2\pi}\Theta[n](\theta)\Theta'[k](\theta)d\theta = \begin{cases} f[n+1] & n\in\{1,3,5,\ldots\} \\ -f[n-1] & n\in\{2,4,6,\ldots\}\end{cases} \quad (66)$$

Thus using (66),(64) can be written as follows,

$$\begin{cases}B_r = \sum_{k=1}^{\infty} B_r[k]\Theta[k](\theta) \\ B_\theta = \sum_{k=1}^{\infty} B_\theta[k]\Theta[k](\theta)\end{cases} \quad (67)$$

where $B_r[k]$ and $B_\theta[k]$ are the respective series coefficients at r=r_g

$$\begin{cases} B_r[n] = \lambda[n]\zeta\left(r^{-1}R[n](r)\right) \\ B_\theta[n] = -R'[n](r) \end{cases} \tag{68}$$

Substituting (67) in (50) using property (62) yields,

$$T_z / \left(\mu_0^{-1} L_z r_g^{\ 2}\right) = \int_0^{2\pi} B_r B_\theta d\theta$$

$$= \int_0^{2\pi} \left(\sum_{n=1}^{\infty} B_r[n]\Theta[n](\theta) \right)\left(\sum_{k=1}^{\infty} B_\theta[k]\Theta[k](\theta) \right) d\theta$$

$$= \sum_{n=1}^{\infty} B_r[n] \sum_{k=1}^{\infty} B_\theta[k] \int_0^{2\pi} \Theta[k](\theta)\Theta[n](\theta) d\theta$$

$$= \sum_{n=1}^{\infty} B_r[n] \sum_{k=1}^{\infty} B_\theta[k]\delta[n,k]$$

$$= \sum_{n=1}^{\infty} B_r[n] B_\theta[n]$$

and thus,

$$T_z = \mu_0^{-1} L_z r_g^{\ 2} \sum_{n=1}^{\infty} B_r[n] B_\theta[n] \tag{69}$$

The force can be derived similarly. In this case, (67) must be substituted in (51),

$$F_x / \left(\mu_0^{-1} L r_g\right) = \int_0^{2\pi} \frac{1}{2}\cos(\theta)\left(B_r^{\ 2} - B_\theta^{\ 2}\right) - \sin(\theta) B_r B_\theta d\theta$$

$$= \left(\begin{aligned} &+\frac{1}{2}\sum_{n=1}^{\infty} B_r[n] \sum_{k=1}^{\infty} B_r[k] \int_0^{2\pi} \cos(\theta)\Theta[k](\theta)\Theta[n](\theta)d\theta \\ &-\frac{1}{2}\sum_{n=1}^{\infty} B_\theta[n] \sum_{k=1}^{\infty} B_\theta[k] \int_0^{2\pi} \cos(\theta)\Theta[k](\theta)\Theta[n](\theta)d\theta \\ &-\sum_{n=1}^{\infty} B_\theta[n] \sum_{k=1}^{\infty} B_r[k] \int_0^{2\pi} \sin(\theta)\Theta[k](\theta)\Theta[n](\theta)d\theta \end{aligned} \right)$$

$$= \frac{1}{2}\sum_{n=1}^{\infty} B_r[n]\eta(B_r[n]) - B_\theta[n]\eta(B_\theta[n]) - 2B_\theta[n]\xi(B_r[n])$$

and,

$$F_y / \left(\mu_0^{-1} L r_g\right) = \int_0^{2\pi} \frac{1}{2}\sin(\theta)\left(B_r^{\ 2} - B_\theta^{\ 2}\right) + \cos(\theta) B_r B_\theta d\theta$$

$$= \frac{1}{2}\left(\begin{aligned} &+\sum_{n=1}^{\infty} B_r[n] \sum_{k=1}^{\infty} B_r[k] \int_0^{2\pi} \sin(\theta)\Theta[k](\theta)\Theta[n](\theta)d\theta \\ &-\sum_{n=1}^{\infty} B_\theta[n] \sum_{k=1}^{\infty} B_\theta[k] \int_0^{2\pi} \sin(\theta)\Theta[k](\theta)\Theta[n](\theta)d\theta \\ &+2\sum_{n=1}^{\infty} B_\theta[n] \sum_{k=1}^{\infty} B_r[k] \int_0^{2\pi} \cos(\theta)\Theta[k](\theta)\Theta[n](\theta)d\theta \end{aligned} \right)$$

$$= \frac{1}{2}\sum_{n=1}^{\infty} B_r[n]\xi(B_r[n]) - B_\theta[n]\xi(B_\theta[n]) + 2B_\theta[n]\eta(B_r[n])$$

Thus

$$\begin{cases} F_x = \mu_0^{-1} L r_g \dfrac{1}{2}\displaystyle\sum_{n=1}^{\infty} \begin{pmatrix} B_r[n]\eta(B_r[n]) - B_\theta[n]\eta(B_\theta[n]) \\ -2B_\theta[n]\xi(B_r[n]) \end{pmatrix} \\ F_y = \mu_0^{-1} L r_g \dfrac{1}{2}\displaystyle\sum_{n=1}^{\infty} \begin{pmatrix} B_r[n]\xi(B_r[n]) - B_\theta[n]\xi(B_\theta[n]) \\ +2B_\theta[n]\eta(B_r[n]) \end{pmatrix} \end{cases} \tag{70}$$

In the above derivation, the following properties were employed,

$$\begin{aligned} \eta(f[n]) &= \sum_{k=1}^{\infty} f[k] \int_0^{2\pi} \cos(\theta)\Theta[n](\theta)\Theta[k](\theta)d\theta \\ &= \frac{1}{2}\left(f[n-2] + f[n+2]\right) \end{aligned} \tag{71}$$

and,

$$\begin{aligned} \xi(f[n]) &= \sum_{k=1}^{\infty} f[k] \int_0^{2\pi} \sin(\theta)\Theta[n](\theta)\Theta[k](\theta)d\theta \\ &= \frac{1}{2}\begin{cases} f[n+3] - f[n-1] & n \in \{1,3,5,\ldots\} \\ f[n-3] - f[n+1] & n \in \{2,4,6,\ldots\} \end{cases} \end{aligned} \tag{72}$$

where $f[n]$ is an arbitrary sequence.

The simple analytic formulas (69) and (70) can be employed to avoid numerical integration, which results in precise computation and very low computational burden. It also gives insight into how the interaction of the harmonic content of the magnetic field distribution in the air gap produces the electromagnetic forces. Additionally, by hybridizing SVM with FEM according to the stress harmonic filter method [4], the obtained formulas can be good candidates for improving accuracy.

7. Application in Mechanical Design

In this section, some of the applications of the formulae derived in this paper are noted for the mechanical design of electromagnetic apparatus. The considerations involved in mechanical design are also pointed out.

The force density formulas derived in Section 2 are the key and the starting point in mechanical robustness analysis. The force density is indeed the input of the mechanical governing equations.

Deformation Analysis

When an external force is applied to a solid, its particles displace in various directions, resulting in a change in the form of the body. When under stress, the solid structure can deform to a degree or even crack; thus, the engineer should estimate the degree of stiffness and deformation. In deformation analysis, displacement, strain and stress of the elastic body under external loadings are analyzed. These determine the final form of the body in the equilibrium state. The recipe of deformation analysis under electromagnetic loading is as follows,

1) *Compute the external force density*: The formulas of force density derived in Section 2 can be used.
2) *Specify the Boundary Conditions*: In the context of elasticity, the boundary conditions are usually in the

form of constraints on force or displacement at the surface. Both types can appear as a result of contact with external rigid bodies; however, a surface force can appear due to magnetic forces as well, which can be obtained using the formulae in Section 2.

3) *Provide the material properties*: The elastic properties, extracted from the stress-strain relationship, include data such as Young's modulus, Poisson's ratio, etc.
4) *Compute Displacements*: Using the knowledge of external force density, boundary conditions and material properties, displacements can be obtained through *Navier-Cauchy equation*.
5) *Post-Processing*: The distribution of stress and strain can be obtained at this stage. Strain is obtained using the spatial derivative of the displacements and the stress is obtained through the stress-strain relationship.

Vibration Analysis

When the external force applied to an elastic solid varies with time, the continuous deformation of the body throughout time results in vibration. The purpose of vibration analysis in the application of electrical machines is two-fold: 1) Fault diagnosis and 2) Study of acoustic noise. The mechanical failure mainly concerns the bearings and the acoustic noise is produced because of the elastic waves induced at the solid surface of the stator. In both cases, the vibration analysis involves a time-variant simulation in steady state (i.e. at constant rotor speed).

The recipe for vibration analysis is as follows,

1) *Compute the external force density*: The formulas of force density derived in Section 2 can be used.
2) *Specify the Boundary Conditions and Initial Conditions*: In the context of wave propagation in elastic media, in addition to surface traction and surface displacement, the constraint on surface velocity is also required for the boundary conditions. The surface velocity is determined via the external contact.
3) *Provide the material properties*: In addition to elastic parameters, other parameters such as mass density and damping properties are required as well.
4) *Compute Displacements*: Using the knowledge of external force density and the material properties, the displacements can be obtained through the *equation of motion* which is the transient form of Navier-Cauchy equation.
5) *Post-Processing*: Velocity and acceleration can be obtained by taking time-derivatives of displacements at this stage.

Alternatively, the equation of motion can be solved in frequency domain. This technique is called *modal decomposition*. The steps involved in modal decomposition are as follows,

1) The displacements are assumed to be composed of a number of *mode shapes*. By substituting these mode shapes in the equation of motion, a system of coupled equations of motion is obtained. The unknowns would then transform into *modal coordinates*.
2) If damping is proportional with mass and stiffness, the coupled system of *modal equations* will be decoupled.
3) Each modal equation (in time domain) can be transformed into the frequency domain by a Fourier transform.
4) After solving each equation of motion in frequency domain, separately, the spectra of individual modes are obtained.
5) By composing the resulting spectra, the actual displacements and accelerations are obtained.

More details about modal decomposition approach can be found at [25] where a coupled magneto-mechanical finite element analysis is conducted.

Magnetostriction Effect

The radial vibration of the stator surface has the most contribution in creating *acoustic noise* in electrical machines. The existence of radial electromagnetic force density is the main cause of radial vibration. However, the *magnetostriction effect* has sometimes significant contribution in radial vibration [25]. The magnetostriction is the effect of magnetization on strain in ferromagnetic bodies. The *inverse magnetostriction* is the dependency of magnetization on normal (tensile/compressive) stress. Therefore the strain will depend on both magnetization and stress. This mutual dependency will inevitably require a magneto-mechanical multi-physics simulation.

8. Fundamental Questions

In this section, some frequently asked questions regarding the fundamental concepts discussed so far are answered in detail.

Question (1):
Magnetostatic forces are generated when magnetic materials and/or steady currents are placed in each other's magnetic field. How can Lorentz force law determine the force to a piece of magnetic material without any current?

Answer:
Magnetic (magnetizable) materials are essentially masses of microscopic current loops called *magnetic dipoles*. These currents exist as a result of the orbital and spinning motions of atomic charges, i.e. electrons and nuclei. Normally, these dipoles have random orientations. The random orientation causes the adjacent dipoles cancel each other out. However, when exposed to external magnetic field, the dipoles align in direction of the magnetic field, resulting in net macroscopic currents. The resulting effective currents are called *bound currents* or *magnetization currents* and are of two types:

- Surface magnetization currents, existing as a surface current density ($\mathbf{J}_{m,s}$)

- Volume magnetization currents, resembling a volume current density ($\mathbf{J}_{m,v}$)

Thus in a way, magnetostatic forces exerted to a magnetic material are Lorentz forces in origin.

Question (2):
Are the magnetization currents mere abstract concepts to represent the magnetic field of a magnetic body or do they physically exist?

Answer:
In engineering community, the magnetization currents are referred to as equivalent currents [14] or virtual currents [26]. This is because in theoretical electromagnetics, the bound currents are derived by pure mathematical manipulation which leaves the impression that they are conceptual. Even a controversial statement is encountered in [14] that "*the equivalent current distributions used to replace the ferromagnetic material preserves the magnetic field external to the material, but not inside the material.*" However, the bound currents are not fictitious and they do possess genuine physical existence [15] as an aggregation of atomic currents as mentioned before.

Question (3):
In all formulae obtained so far, there is no direct indication of material properties. Where is the impact of material properties?

Answer:
The answer is twofold:
1) *Formulas Based on Lorentz Force Law*
To compute force using the Lorentz force law, the total magnetic field **B**

$$\nabla \times \mathbf{B} = \mu_0 \mathbf{J} \tag{73}$$

as well as the total current **J**

$$\mathbf{J} = \mathbf{J}_f + \mathbf{J}_m \tag{74}$$

must be known, where the total current is the sum of two types of current sources,

- Applied or free currents $\mathbf{J}_f$: can be viewed as independent current sources
- Magnetization currents $\mathbf{J}_m$: can be viewed as dependent current sources

The bound currents $\mathbf{J}_m$ are controlled by the total magnetic field **B**. The intrinsic material properties determine how $\mathbf{J}_m$ is related to **B**. Therefore, the influence of properties such as nonlinearity, inhomogeneity and anisotropicity are all contained within **J** and **B**. However, $\mathbf{J}_m$ is often not directly accessible and **J** is not explicitly known, therefore **J** is written in terms of **B** using (73). In formulas written in terms of purely magnetic field, the account of material properties is thereby embedded in **B**.
2) *Formulas Based on Principle of Conservation of Energy*
The energy balance equation provides a relation between the electrical energy, the energy stored in the magnetic field and the mechanical energy. The electrical energy indicates the electrical energy that is transferred in to or out of the system not floating in the magnetic field. Therefore the free currents are considered in energy formula not the magnetization currents. The impact of magnetization is *seen* in the magnetic field.

Question (4):
What principle to use? The Lorentz force or the Conservation energy?

Answer:
Both laws are based on solemn physical principles and have the same results, theoretically. It is only the computational approach that makes distinction in practice. TABLE. 1 gives an insightful comparison.

Question (5):
What is the point in introducing Maxwell stress tensor and the Maxwell couple stress tensor? Wasn't it easier to use the force density formula derived from Lorentz force law?

Answer:
The divergence of the Maxwell stress tensor is equal to the volume force density and the divergence of the Maxwell couple stress tensor equals the torque density. For computing the resultant force and the net torque, these enable the application of the divergence theorem which reduces the volume integral to a surface integral. Therefore, they are endowed with a computational advantage.

TABLE. 1. Comparison of Stress Method and Co-energy (Virtual Work) Method For Force Computation

Maxwell Stress Tensor/ Maxwell Couple Stress Tensor	Co-energy (Virtual Work)
Does not require additional time integration for non-linear media[23]	For non-linear media requires an additional time integration
Always computed by surface integral on a cylindrical shell in air gap	In general, requires volume integration throughout the conductors or magnets
Computational complexity does not depend on geometry	Volume integration becomes difficult for complicated geometry
Requires the spatial derivative of the potential that can be obtained analytically	Requires numerical derivative with respect to rotor position
Calculation of radial forces is as simple as for computation of torque	Becomes very difficult for calculation of unbalanced forces
in a rigorous mathematical sense, localization to surface traction is incorrect but the results are often in good agreement with experimental data	Reyne stress method as a modified form of Maxwell stress tensor based on energy concept is proposed to account for local stress vector
Accurate for analytical methods such as SVM (Harmonic or Fourier models); because the solutions exactly satisfy field equations	Accurate for FEM; because formulation of FEM is based on energy and thereby the total energy is obtained very accurately[23]

Question (6):
Is it correct to conclude that the Maxwell stress tensor and the Maxwell couple stress tensor are the actual surface force density?

Answer:
No, it is not. The integration of Maxwell stress tensor and the Maxwell couple stress tensor over a closed surface yields the resultant force and the net torque to the volume. If the surface of integration is reduced to a point, the surface is still closed. However, the surface force density is defined across an open flat surface. Moreover, the magnetic surface force density is only nonzero at the surface of a magnetic material or at a current sheet. Furthermore, stress is a quantity that is determined only by the mechanical response of the material, not just by magnetic field.

Question (7):
Is Maxwell stress tensor coordinate-independent?

Answer:
No, it is not. In Appendix 2-Theorem (5), it is proved for e.g. cylindrical coordinates. Some authors, e.g. [5] mistakenly generalize (19) for any coordinates system by just replacing the indices with any arbitrary coordinates system.

9. VALIDATION AND CASE-STUDY

In order to verify both the validity and the applicability of the formulas, three case-studies are investigated in this section.

Case-Study (1): *Coreless Machine*

Fig. 9 shows a conceptual machine: a coreless machine with ideal single harmonic volume current density distribution $\mathbf{J}_{v,z}$ in both rotor and stator; i.e.,

$$\begin{cases} J_{v,z1}(\theta) = J_1 \cos(\theta - \theta_r) \\ J_{v,z2}(\theta) = J_2 \cos(\theta) \end{cases} \tag{75}$$

where the subscripts 1 and 2 denote the rotor and stator, respectively and θ_r is the rotor position. The machine can be thought of as a continuously distributed sinusoidal winding.

In this special case, it is possible to obtain the field distribution analytically in closed-form in all regions. SVM can be employed for this purpose where a set of general solutions is derived for Laplace and Poisson equations for all sub-domains and then using their interface conditions, the particular solution is obtained. If the procedure is followed, one can obtain the electromagnetic torque as follows,

$$T_z = -\frac{\pi}{6} L_z \mu_0 J_1 J_2 \left(r_{b2}^{\ 3} - r_{b1}^{\ 3}\right)\left(r_{b4} - r_{b3}\right)\sin(\theta_r) \tag{76}$$

It has been shown that the methods of Lorentz force in its raw form (3), the couple stress vector (38), (50) or (69) and the co-energy method (42) lead to the above result. Therefore in theory, all formulas for both methods of force calculation should lead to the same result. In addition, the net force to the rotor has been evaluated exactly zero.

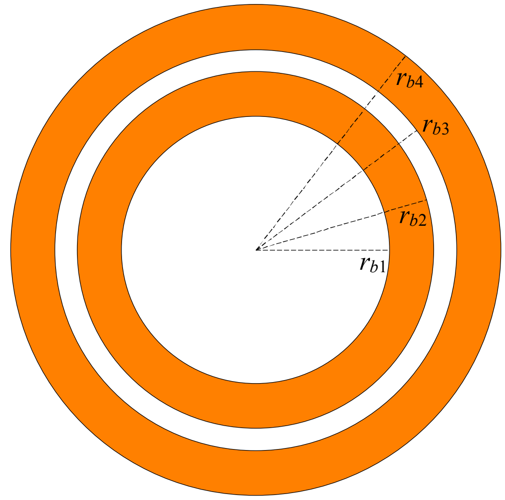

Fig. 9. Conceptual coreless machine. Both rotor and the stator consist of a cylinder of current with spatially sinusoidal distribution of volume current density across azimuthal direction.

Case-Study (2): *Current-Sheet Machine*

To account for surface currents and ferromagnetic effects, a second conceptual machine is studied: Fig. 10 shows a smooth air gap machine with current sheet windings on both stator and rotor. The back-irons are assumed to be perfect ferromagnetic materials. The surface current distribution is assumed ideal single harmonic.

$$\begin{cases} J_{s,z1}(\theta) = J_1 \cos(\theta - \theta_r) \\ J_{s,z2}(\theta) = J_2 \cos(\theta) \end{cases} \tag{77}$$

where the subscripts 1 and 2 denote the rotor and stator, respectively.

In this special case, the analytical solution is derived exactly in closed-form, which makes it possible for an exact validation.

$$T_z = -\frac{r_{b3}^{\ 2} r_{b2}^{\ 2}}{r_{b3}^{\ 2} - r_{b2}^{\ 2}} 2\pi L_z \mu_0 J_1 J_2 \sin(\theta_r) \tag{78}$$

This result has been equal for all of these methods:

- Lorentz force law using current density
- Couple stress vector in the air-gap
- Integration of surface force density
- Energy method

The net force to the rotor has also been evaluated as exactly zero.

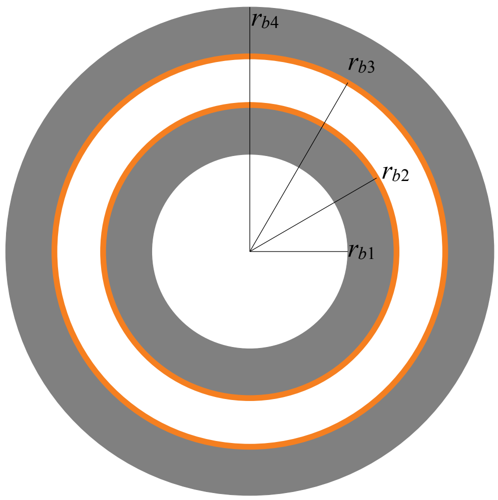

Fig. 10. Conceptual current-sheet machine. Both stator and rotor consist of a perfect ferromagnet (gray) and a thin layer of current tape (orange). The surface current density is assumed to be distributed pure sinusoidally across azimuthal direction.

Case-Study (3): *Slotted Iron-cored Surface Magnet Machine*

The very first and second case-studies were only a means of theoretical validation of the discussed methods. In practice, electrical machines have complicated geometrical ferromagnetic cores. Thus a third case-study shown in Fig. 11 is investigated. For this case, SVM as a semi-analytical method can be employed to accurately obtain the magnetic field in active parts of the machine (windings/magnets and air-gap).

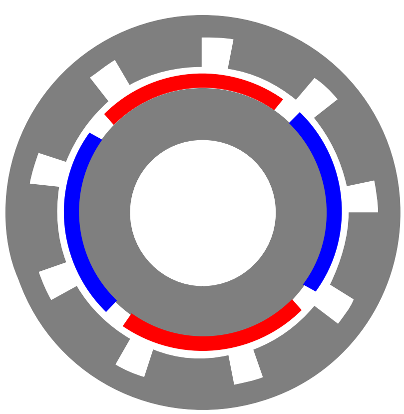

Fig. 11. Slotted surface magnet machine.

SVM was employed to obtain the magnetic field distribution of air-gap in the form of Fourier series (67). Thus the formulas based on Lorentz force law developed for harmonic model, i.e. (69) and (70) could be employed. The computational time has been recorded approximately 0.01 seconds. The same method was first conducted using numerically integrating (50) and (51) and it took 0.7 seconds.

Since linear materials were used in this study, the co-energy was obtained using (58) in which the magnetization currents of the magnets were computed using (47). Then the cogging torque was obtained by numerically derivation of co-energy with respect to rotor position (59). This method has taken approximately 0.3 seconds in which both integration (trapezoidal rule) and derivation (central finite difference) were performed numerically. It is noted that the integration can be performed analytically in certain cases but not always.

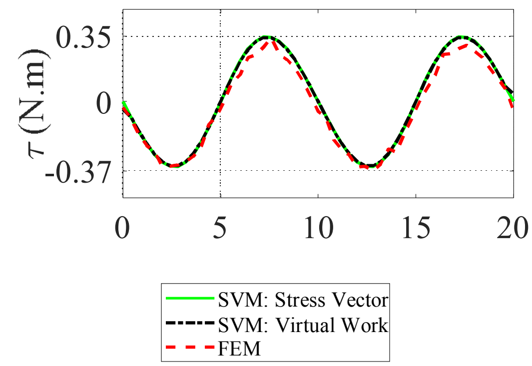

Fig. 12. Cogging torque (Nm) of the second case-study per unit axial length (1 meter) versus rotor displacement θ_r (deg.). The SVM: Stress Vector result is obtained by (69) which is a result of (50) whereas the SVM: Virtual Work result is obtained by (59).

The results of the third case-study with the parameters given in TABLE 2 have been derived and depicted in Figs. 12-15.

Fig. 12 shows the cogging torque and Fig. 13 shows the cog attraction force to the rotor. As observed, the results are in good agreement with the results obtained by the FEM software. This case has a large cog attraction force because the greatest common divisor of the number of slots and the number of poles equals one [22].

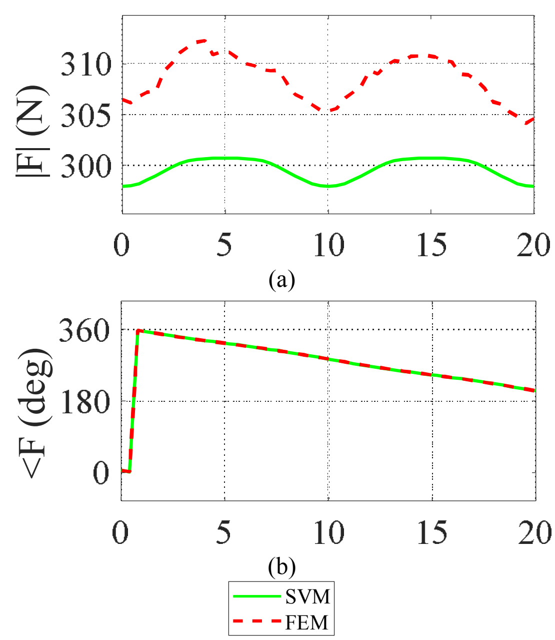

Fig. 13. a) Magnitude (N) and b) angle (deg.) of the unbalanced (resultant) force exerted to the rotor of the machine in Fig. 11 per unit axial length (1 meter) versus rotor position θ_r (deg.). The SVM results are obtained via the formula of (70) which is a result of (51).

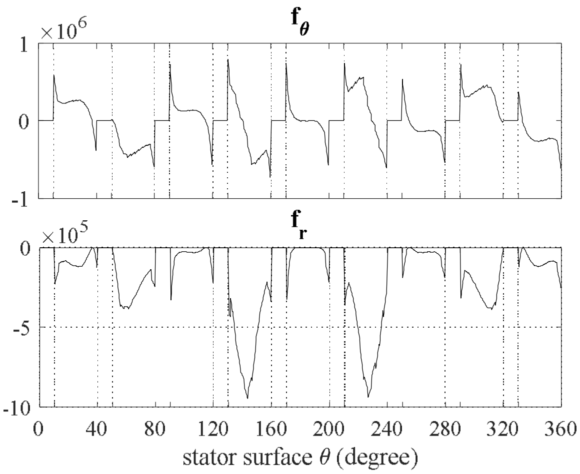

Fig. 14. Surface force density (N/m^2) at the circumference of stator teeth using the relations (48) and (49). The force density at the surface of slots is obviously zero.

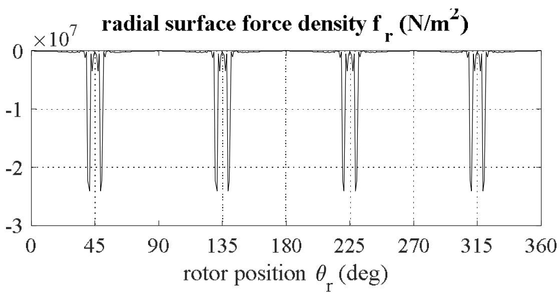

Fig. 15. The radial component of surface force density (N/m^2) at the middle of one stator tooth against an entire revolution of the rotor. The attraction force surges when the middle point of the poles is about to face the considered tooth.

Fig. 14 can be used for deformation analysis. It shows the surface force density distribution at the surface of the stator teeth. The results are obtained by post-processing the magnetic field obtained by FEM. The radial force is always negative, showing that the cog force is attractive and never repulsive. The tangent force, however, oscillates as the distribution of reluctance is non-uniform.

Fig. 15 is the vibrating electromagnetic force. It shows the radial force density on a fixed point at the surface of a stator tooth. As the rotor rotates, this force varies which results in vibration of the stator yoke. The spikes of the graph are produced at every mechanical pole-pitch (here 90 degrees for the 4-pole machine). Indeed, these peaks arise when the middle point between two adjacent poles faces the stator tooth. This point creates the strongest surface force density the machine can produce.

TABLE. 2. Case-study Parameters

Outer radius of rotor shaft (r_{b2})	10 mm
Outer radius of rotor back-iron (r_{b3})	17 mm
Outer radius of PMs (r_{b4})	19 mm
Outer radius of air-gap (r_{b5})	20 mm
Outer radius of slots/teeth (r_{b6})	24 mm
Outer radius of stator back-iron (r_{b7})	27 mm
Stator slot span to slot-pitch ratio (α_{sl})	0.26
PM width to pole-pitch ratio (α_{PM})	0.9
Number of stator slots	9
Number of magnetic poles (=permanent magnets)	4
Ferromagnetic material relative permeability ($\mu_{r,FM}$)	1000
Permanent magnets relative (recoil) permeability ($\mu_{r,PM}$)	1
Permanent magnet remanent flux density (B_{rem})	1 T

10. Summary and Concluding Remarks

Advanced magnetic modeling methods can accurately estimate the magnetic field distribution in electrical machinery. The obtained magnetic field, however, should be carefully post-processed to efficiently and precisely predict the motor parameters, most importantly, the electromagnetic forces. The purpose of this paper was to review the methods of force calculation in electrical machines. A few expressions were obtained both in general and simplified forms using the Lorentz force law and the principle of conservation of energy. The energy method is best suited for FEM, whereas the formulations based on the Lorentz force law are best suited for methods with high magnetic field accuracy. For brevity, some of the key formulae are repeated here,

- The surface force density $\mathbf{f}_s$, where $\mathbf{a}_n$ is the normal unit vector pointing from side "2" to side "1" of an interface with a discontinuous magnetic field

$$\mathbf{f}_s = \frac{1}{2}\mu_0^{-1}\left(\mathbf{a}_n \times \left(\mathbf{B}_1 - \mathbf{B}_2\right)\right) \times \left(\mathbf{B}_1 + \mathbf{B}_2\right) \quad (79)$$

- The volume force density $\mathbf{f}_v$

$$\mathbf{f}_v = \mu_0^{-1}\left(\nabla \times \mathbf{B}\right) \times \mathbf{B} \quad (80)$$

- The volume torque density vector $\boldsymbol{\tau}$, where $\mathbf{r}$ is the location vector, i.e. the distance of the volume element to the origin

$$\boldsymbol{\tau} = \mu_0^{-1}\mathbf{r} \times \left(\left(\nabla \times \mathbf{B}\right) \times \mathbf{B}\right) \quad (81)$$

- The surface force density in terms of the Maxwell stress tensor $\boldsymbol{\sigma}$

$$\mathbf{f}_s = \left(\boldsymbol{\sigma}_1 - \boldsymbol{\sigma}_2\right) \cdot \mathbf{a}_n \quad (82)$$

- The volume force density in terms of the Maxwell stress tensor

$$\mathbf{f}_v = \nabla \cdot \boldsymbol{\sigma} \quad (83)$$

- The volume torque density vector in terms of the Maxwell couple stress tensor **m**,

$$\boldsymbol{\tau} = \nabla \cdot \mathbf{m} \tag{84}$$

- The resultant force to a system enclosed by the surface *S*,

$$\mathbf{F} = \oint_S \boldsymbol{\sigma} \cdot d\mathbf{s} \tag{85}$$

- The net torque vector **T** to a system enclosed by the surface *S*,

$$\mathbf{T} = \oint_S \mathbf{m} \cdot d\mathbf{s} \tag{86}$$

REFERENCES

[1] YAN, Xiuke, TI, "Comparison of Force Calculation Methods in 2D and 3D Finite Element Method", *KIEE International Tran on EMECS*, vol. 11, pp. 137-145, 2001.

[2] Y. Okamoto, T. Iino and A. Ahagon, "Error Correction of Electromagnetic Force Calculation Using Nodal Force Method in Time Domain Eddy Current Analysis," 2022 IEEE 20th Biennial Conference on Electromagnetic Field Computation (CEFC), Denver, CO, USA, 2022, pp. 1-2, doi: 10.1109/CEFC55061.2022.9940816.

[3] S. Elia, M. Pasquali, G. Remigi, M.V. Sabene& E. Santini, "A modified Maxwell stress tensor method for the evaluation of electromagnetic torque", *WIT Transactions on Engineering Sciences*, vol. 31, p. 10, 2001. Paper DOI: 10.2495/ES010031.

[4] M. Popescu, "Prediction of the electromagnetic torque in synchronous machines through Maxwell stress harmonic filter (HFT) method", Electr. Eng., vol. 89, pp. 117–125, 2006. https://doi.org/10.1007/s00202-005-0323-1.

[5] K. J. Meessen, J. J. H. Paulides and E. A. Lomonova, "Force Calculations in 3-D Cylindrical Structures Using Fourier Analysis and the Maxwell Stress Tensor," *IEEE Transactions on Magnetics*, vol. 49, no. 1, pp. 536-545, Jan. 2013, doi: 10.1109/TMAG.2012.2206821.

[6] D. Zarko, D. Ban and T. A. Lipo, "Analytical Solution for Cogging Torque in Surface Permanent-Magnet Motors Using Conformal Mapping," *IEEE Transactions on Magnetics*, vol. 44, no. 1, pp. 52-65, Jan. 2008, doi: 10.1109/TMAG.2007.908652.

[7] W. Tong, S. Li, X. Pan, S. Wu and R. Tang, "Analytical Model for Cogging Torque Calculation in Surface-Mounted Permanent Magnet Motors With Rotor Eccentricity and Magnet Defects," *IEEE Transactions on Energy Conversion*, vol. 35, no. 4, pp. 2191-2200, Dec. 2020, doi: 10.1109/TEC.2020.2995902.

[8] Y. Zhu, G. Liu, L. Xu, W. Zhao and D. Cao, "A Hybrid Analytical Model for Permanent Magnet Vernier Machines Considering Saturation Effect," *IEEE Transactions on Industrial Electronics*, vol. 69, no. 2, pp. 1211-1223, Feb. 2022, doi: 10.1109/TIE.2021.3060656.

[9] W. Liu, H. Yang, H. Lin and L. Qin, "Hybrid Analytical Modeling of Air-Gap Magnetic Field in Asymmetric-Stator-Pole Flux Reversal Permanent Magnet Machine Considering Slotting Effect," *IEEE Transactions on Industrial Electronics*, vol. 69, no. 2, pp. 1739-1749, Feb. 2022, doi: 10.1109/TIE.2021.3062265.

[10] A. Rahideh and T. Korakianitis, "Analytical Open-Circuit Magnetic Field Distribution of Slotless Brushless Permanent-Magnet Machines With Rotor Eccentricity," *IEEE Transactions on Magnetics*, vol. 47, no. 12, pp. 4791-4808, Dec. 2011, doi: 10.1109/TMAG.2011.2159987.

[11] A. Rahideh, and T. Korakianitis. "Analytical Magnetic Field Distribution of Slotless Brushless PM Motors. Part 2: Open-Circuit Field and Torque Calculations." *IET Electric Power Applications*, vol. 6, no. 9, 2012, p. 639, https://doi.org/10.1049/iet-epa.2011.0386.

[12] Pile, R., Besnerais, J. L., Parent, G., Devillers, E., Henneron, T., Menach, Y. L., & Lecointe, J. (2020). Analytical study of air-gap surface force – application to electrical machines. Open Physics, 18(1), 658–673. https://doi.org/10.1515/phys-2020-0147

[13] D. K. Cheng, *Field and Wave Electromagnetics*, Addison-Wesley, 2nd edition, 1989.

[14] S.R.H. Hoole, *Finite Elements, Electromagnetics and Design*, Elsevier Science, 1st edition, 1995.

[15] D. J. Griffiths, *Introduction to Electrodynamics*, Pearson Education Inc., 4th Edition, 2013.

[16] Carpenter, C.J. "Surface-Integral Methods of Calculating Forces on Magnetized Iron Parts." Proceedings of the Institution of Electrical Engineers. Part C, Monographs, vol. 107, no. 11, 1 Jan. 1960, pp. 19–19, https://doi.org/10.1049/pi-c.1960.0005.

[17] J. R. Brauer, *Magnetic Actuators and Sensors*, Wiley-IEEE Press, 2006.

[18] S. J. Chapman, *Electric Machinery Fundamentals*, McGraw-Hill, 5th edition.

[19] P.C. Sen, *Principles of Electric Machines and Power Electronics*, John Wiley and Sons, 2nd edition, 1996.

[20] J.F. Gieras and M. Wing, *Permanent Magnet Motor Technology Design and Applications*, 2nd edition, 2002.

[21] M. H. Javanmardi, A. Rahideh and V. Z. Faradonbeh, "Analytical Cogging Torque and Unbalanced Magnetic Force Calculations in Slotted Surface-PM Machines Assuming Finite Iron Permeability," *IEEE Transactions on Transportation Electrification*, doi: 10.1109/TTE.2024.3365137.

[22] D. Hanselman, *Brushless Permanent Magnet Motor Design*, 2nd edition, 2006.

[23] K. Hameyer*et al*, *Numerical Modelling and Design of Electrical Machines and Devices*, WIT Press, 1999.

[24] Mörée, G., & Leijon, M. (2023). The force density in electrical machines modeled as tension and pressure gradients of magnetic field lines. AIP Advances, 13(2). https://doi.org/10.1063/5.0122245

[25] Finite Element Analysis of Electrical Machine Vibrations caused by Lorentz, Maxwell and Magnetostriction Forces

[26] F. Farrokh, A. Vahedi, H. Torkaman, M. Banejad and V. Zamani Faradonbeh, "Fast 2-D Analytical Model for Axial-Field Flux-Switching Bar-Permanent Magnet Motor," in IEEE Transactions on Magnetics, vol. 60, no. 8, pp. 1-12, Aug. 2024, Art no. 8201912, doi: 10.1109/TMAG.2024.3416176.

[27] M. H. Sadd, *Elasticity, Theory, Applications and Numerics*, Academic Press, 2nd edition, 2009.

APPENDIX 1: MEAN FLUX DENSITY THEOREM

In Section 2, an expression (6) for the surface force density at a current sheet was derived purely in terms of magnetic flux density. Due to the discontinuity of the flux density at the surface of the current sheet, the magnetic flux density was averaged. At first thought, the average sense might seem only a simple means to obtain a unique value. However, the idea of averaging is correct and there is a concrete physical proof for it. In this paper, this fact is named as the title of this appendix, the *Mean Flux Density Theorem*. In this section, the mean flux density theorem is proved using rigorous mathematical expressions.

Theorem (1): *Mean Flux Density at Surface Currents*

Assume a current-carrying sheet with surface current density $\mathbf{J}_s$. Consider an element of surface *ds* at point *P* on the current sheet. Define the external magnetic flux density $\mathbf{B}_{ext}$ as the magnetic field created by all other nearby surface elements plus all other sources of current at all space. The external magnetic field is the mean of the pair of values, $\mathbf{B}_1$ and $\mathbf{B}_2$, of the discontinuous magnetic field on both sides of the current sheet at *P*.

$$\mathbf{B}_{ext} = \frac{1}{2}(\mathbf{B}_1 + \mathbf{B}_2) \quad (87)$$

This theorem is valuable in view of extracting the external component of the magnetic field for the purpose of post-processing.

Proof:

At the point P, the magnetic field on both sides can be stated as the superposition of two contributions:

1) $\mathbf{B}_{ds}$ created by $\mathbf{dI} = \mathbf{J}_s dw$, the differential current of the surface element ds, where dw is the width of ds.
2) $\mathbf{B}_{ext}$ resembles all other contributions except the one created by $\mathbf{dI} = \mathbf{J}_s dw$.

$\mathbf{B}_{ext}$ is continuous on both sides of the current sheet, whereas $\mathbf{B}_{ds}$ is discontinuous. Due to the perfect symmetry of the distribution of $\mathbf{B}_{ds}$, the magnitudes of $\mathbf{B}_{ds}$ are identical on both sides, but their directions are opposite each other.

Therefore, the total magnetic field at the point P on the current sheet can be written as follows:

$$\begin{cases} \mathbf{B}_1 = \mathbf{B}_{ext} - \mathbf{B}_{ds} \\ \mathbf{B}_2 = \mathbf{B}_{ext} + \mathbf{B}_{ds} \end{cases} \quad (88)$$

The objective is now to extract $\mathbf{B}_{ext}$. Once the field solution is known, the total magnetic fields at both sides of the current sheet, i.e. $\mathbf{B}_1$ and $\mathbf{B}_2$, are known. $\mathbf{B}_{ext}$ and $\mathbf{B}_{ds}$ are thereby the unknowns of the simultaneous equations of (88). Solving the equations,

$$\mathbf{B}_{ext} = \frac{1}{2}(\mathbf{B}_1 + \mathbf{B}_2) \quad (89)$$

Equation (89) states that the contribution of all sources of magnetic field at a particular point on a current sheet, excluding the contribution of the differential current of the surface element at that point, is the mean value of the discontinuous values of magnetic field at both sides of the current sheet.

Theorem (2)*: Flux Density at the Center of a Square-shaped Current Sheet*

Assume a square sheet lying on x-z plane and bearing a surface current density $\mathbf{J}_s = J_s \mathbf{a}_z$ (Fig. 16). The value of the magnetic field at the center of the current sheet is independent of the size of the sheet and is given by,

$$\lim_{h \to 0} \mathbf{B}(x = 0, y = \pm h, z = 0) = \frac{\mp \mu_0 J_s}{2} \mathbf{a}_x \quad (90)$$

Proof:

The coordinates of the source point and field point are respectively notated with Greek and Latin letters,

$$\begin{cases} \mathbf{x} = x\mathbf{a}_x + y\mathbf{a}_y + z\mathbf{a}_z \\ \boldsymbol{\xi} = \xi\mathbf{a}_x + \eta\mathbf{a}_y + \zeta\mathbf{a}_z \end{cases}$$

The size of the square sheet is assumed as follows,

$$\begin{cases} -L/2 < \xi < +L/2 \\ -L/2 < \zeta < +L/2 \end{cases}$$

According to Biot-Savart's law,

$$\mathbf{B}(\mathbf{x}) = \int_S \frac{-1}{4\pi} \frac{\mathbf{x} - \boldsymbol{\xi}}{|\mathbf{x} - \boldsymbol{\xi}|^3} \times \mu_0 \mathbf{J}_s ds$$

$$= \frac{-\mu_0 J_s}{4\pi} \int_{-L/2}^{+L/2} \int_{-L/2}^{+L/2} \frac{\left((x-\xi)\mathbf{a}_x + y\mathbf{a}_y + (z-\zeta)\mathbf{a}_z\right) \times \mathbf{a}_z}{\left((x-\xi)^2 + y^2 + (z-\zeta)^2\right)^{3/2}} d\xi d\zeta$$

$$= \frac{-\mu_0 J_s}{4\pi} \int_{-L/2}^{+L/2} \int_{-L/2}^{+L/2} \frac{y\mathbf{a}_x - (x-\xi)\mathbf{a}_y}{\left((x-\xi)^2 + y^2 + (z-\zeta)^2\right)^{3/2}} d\xi d\zeta$$

The z-component is zero in the entire space,

$$B_z(x, y, z) = 0$$

The magnetic field on the direction perpendicular to the current sheet (y-axis) is of interest,

$$\mathbf{B}(x = 0, y, z = 0)$$

$$= \frac{-\mu_0 J_s}{4\pi} \int_{-L/2}^{+L/2} \int_{-L/2}^{+L/2} \frac{y\mathbf{a}_x + \xi\mathbf{a}_y}{\left(\xi^2 + y^2 + \zeta^2\right)^{3/2}} d\xi d\zeta$$

The y-component on the whole y-axis is zero, because the integrand has the property of odd-symmetry,

$$B_y(x = 0, y, z = 0)$$

$$= \frac{-\mu_0 J_s}{4\pi} \int_{-L/2}^{+L/2} \int_{-L/2}^{+L/2} \frac{\xi}{\left(\xi^2 + y^2 + \zeta^2\right)^{3/2}} d\xi d\zeta = 0$$

As for the x-component on the y-axis, an analytical evaluation can be derived,

$$B_x(x = 0, y, z = 0)$$

$$= \frac{-\mu_0 J_s}{4\pi} \int_{-L/2}^{+L/2} \int_{-L/2}^{+L/2} \frac{y}{\left(\xi^2 + y^2 + \zeta^2\right)^{3/2}} d\xi d\zeta$$

$$= \frac{-\mu_0 J_s}{4\pi} \arctan\left(\frac{\xi\zeta}{y\sqrt{\zeta^2 + y^2 + \xi^2}} \right) \Bigg|_{\xi=-L/2}^{\xi=+L/2} \Bigg|_{\zeta=-L/2}^{\zeta=+L/2}$$

$$= \frac{-\mu_0 J_s}{\pi} \arctan\left(\frac{(L/2)^2}{y\sqrt{2(L/2)^2 + y^2}} \right)$$

It is now possible to evaluate the limit of the expression as y approaches zero,

$$\lim_{h \to 0} B_x(x = 0, y = \pm h, z = 0) = \frac{\mp \mu_0 J_s}{2}$$

Combining the above results for B_x, B_y, and B_z gives (90).

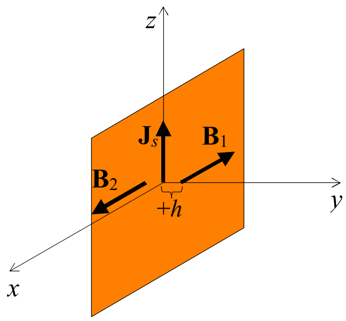

Fig. 16. An $L\times L$ square-shaped current sheet on xz plane with surface current density $\mathbf{J}_s$ in $+z$ direction. $\mathbf{B}_1$ and $\mathbf{B}_2$ are the discontinuous flux density vectors above (y=+h) and below (y=−h) the surface at the center (x=y=0).

Verification of Mean Flux Density Theorem

Solving the system (88) also yields $\mathbf{B}_{ds}$ in terms of $\mathbf{B}_1$ and $\mathbf{B}_2$,

$$-2\mathbf{B}_{ds} = (\mathbf{B}_1 - \mathbf{B}_2) \tag{91}$$

and substituting (91) in (4) gives the value of $\mathbf{B}_{ds}$.

$$\mathbf{a}_{n,2} \times \mathbf{B}_{ds} = \frac{-\mu_0 \mathbf{J}_s}{2} \tag{92}$$

The above expression can be verified using Biot-Savart's law. It is given in the form of Theorem (2). As evident in (90), the $\mathbf{B}$ at the central point of the square current sheet only depends on the surface current density $\mathbf{J}_s$. Irrespective of L, the size of the square-shaped current sheet, the limit approaches a finite value. This shows that the above evaluations are valid for an arbitrarily small square, i.e. a differential element of surface ds.
Previously, the fact that $\mathbf{B}_{ds}$ preserves magnitude but changes direction was used in the proof of Theorem (1) by the intuition of the field distribution symmetry. This intuition is now proved in Theorem (2) and is evident in (90).

Furthermore, if the region of y>0 is chosen as the subspace 1, then according to (88), $\mathbf{B}_{ds}$ refers to subspace 2 (where y<0) and using (90) it is given by,

$$\mathbf{B}_{ds} = \left(B_x\mathbf{a}_x + B_y\mathbf{a}_y + B_z\mathbf{a}_z\right)\Big|_{y=-h} = \frac{+\mu_0 J_s}{2}\mathbf{a}_x$$

Substituting the above relation in (92),

$$\mathbf{a}_{n,2} \times \mathbf{B}_{ds} = \mathbf{a}_y \times \frac{\mu_0 J_s}{2}\mathbf{a}_x = \frac{-\mu_0 J_s \mathbf{a}_z}{2} = \frac{-\mu_0 \mathbf{J}_s}{2}$$

shows the compatibility of relation (92) – which was derived by intuition – with (90) – which is a concrete assertion that was obtained by field solution.

It might be surprising that although it is created from a differential current ($d\mathbf{I}$ = $\mathbf{J}_s dw$), $\mathbf{B}_{ds}$ is finite and not differential. The reason of this surprising phenomenon lies in the fact that the distance of field point P to the surface element ds (source point) is zero. In fact, $d\mathbf{I}$ = $\mathbf{J}_s dw$ which occurs on ds is the only source of discontinuity. Had $\mathbf{B}_{ds}$ not been finite, flux would have become continuous, $\mathbf{B}_1$=$\mathbf{B}_2$.

APPENDIX 2: VECTOR ANALYSIS

In this appendix, some of the mathematical prerequisites regarding vector analysis are reviewed. The supplementary material is indispensable for analysis of the formulae given in this paper. Engineers who are unaccustomed with this topic can use this appendix without having to refer to text books.

Additionally, the procedure to obtain the Maxwell stress tensor and the Maxwell couple stress tensor are given in detail.

Notation Remark

vector fields, whether in rectangular or cylindrical coordinates are notated with column vectors.

- in rectangular coordinates

$$\mathbf{B} = B_x\mathbf{a}_x + B_y\mathbf{a}_y + B_z\mathbf{a}_z = \begin{bmatrix} B_x \\ B_y \\ B_z \end{bmatrix} \tag{93}$$

- in cylindrical coordinates

$$\mathbf{B} = B_r\mathbf{a}_r + B_\theta\mathbf{a}_\theta + B_z\mathbf{a}_z = \begin{bmatrix} B_r \\ B_\theta \\ B_z \end{bmatrix} \tag{94}$$

where $\mathbf{a}_i$ is the unit vector in i-direction.

Product of Vectors

For two vectors, two types of products are defined:

1) Scalar Product (aka inner or dot): gives a scalar
2) Vector Product (aka outer or cross): gives a vector perpendicular to both vectors.

The definitions are tabulated in TABLE. 3.

TABLE. 3. Products of two arbitrary vectors **A** and **B** in rectangular/cylindrical coordinates.

Vector Product $\mathbf{A}\times\mathbf{B}$	Scalar Product $\mathbf{A}\cdot\mathbf{B}$	
$\begin{bmatrix} A_yB_z - A_zB_y \\ A_zB_x - A_xB_z \\ A_xB_y - A_yB_x \end{bmatrix}$	$A_xB_x + A_yB_y + A_zB_z$	Rectangular Coordinates
$\begin{bmatrix} A_\theta B_z - A_zB_\theta \\ A_zB_r - A_rB_z \\ A_rB_\theta - A_\theta B_r \end{bmatrix}$	$A_rB_r + A_\theta B_\theta + A_zB_z$	Cylindrical Coordinates

Derivative of Vector Fields

For vector fields, two types of derivatives are defined:

3) Divergence: gives a scalar field
4) Curl: gives a vector field.

The definitions are tabulated in TABLE. 4.

TABLE. 4. Vector derivatives in rectangular/cylindrical coordinates.

Curl $\nabla\times\mathbf{B}$	Divergence $\nabla\cdot\mathbf{B}$	
$\begin{bmatrix} \frac{\partial B_z}{\partial y}-\frac{\partial B_y}{\partial z} \\ \frac{\partial B_x}{\partial z}-\frac{\partial B_z}{\partial x} \\ \frac{\partial B_y}{\partial x}-\frac{\partial B_x}{\partial y} \end{bmatrix}$	$\frac{\partial B_x}{\partial x}+\frac{\partial B_y}{\partial y}+\frac{\partial B_z}{\partial z}$	Rectangular Coordinates
$\begin{bmatrix} \frac{1}{r}\frac{\partial B_z}{\partial \theta}-\frac{\partial B_\theta}{\partial z} \\ \frac{\partial B_r}{\partial z}-\frac{\partial B_z}{\partial r} \\ \left(\frac{1}{r}+\frac{\partial}{\partial r}\right)B_\theta-\frac{1}{r}\frac{\partial B_r}{\partial \theta} \end{bmatrix}$	$\left(\frac{1}{r}+\frac{\partial}{\partial r}\right)B_r+\frac{1}{r}\frac{\partial B_\theta}{\partial \theta}+\cdots$	Cylindrical Coordinates

Theorem (3): *Decomposing the volume force density to tension and pressure gradient forces*

$$(\nabla\times\mathbf{B})\times\mathbf{B}=(\mathbf{B}\cdot\nabla)\mathbf{B}-\frac{1}{2}\nabla|\mathbf{B}|^2 \tag{95}$$

Proof:

$$(\nabla\times\mathbf{B})\times\mathbf{B}$$

$$=\begin{bmatrix} \frac{\partial B_z}{\partial y}-\frac{\partial B_y}{\partial z} \\ \frac{\partial B_x}{\partial z}-\frac{\partial B_z}{\partial x} \\ \frac{\partial B_y}{\partial x}-\frac{\partial B_x}{\partial y} \end{bmatrix}\times\begin{bmatrix} B_x \\ B_y \\ B_z \end{bmatrix}$$

$$=\begin{bmatrix} \left(\frac{\partial B_x}{\partial z}-\frac{\partial B_z}{\partial x}\right)B_z-\left(\frac{\partial B_y}{\partial x}-\frac{\partial B_x}{\partial y}\right)B_y \\ \left(\frac{\partial B_y}{\partial x}-\frac{\partial B_x}{\partial y}\right)B_x-\left(\frac{\partial B_z}{\partial y}-\frac{\partial B_y}{\partial z}\right)B_z \\ \left(\frac{\partial B_z}{\partial y}-\frac{\partial B_y}{\partial z}\right)B_y-\left(\frac{\partial B_x}{\partial z}-\frac{\partial B_z}{\partial x}\right)B_x \end{bmatrix}$$

$$=\begin{bmatrix} \frac{\partial B_x}{\partial z}B_z+\frac{\partial B_x}{\partial y}B_y \\ \frac{\partial B_y}{\partial x}B_x+\frac{\partial B_y}{\partial z}B_z \\ \frac{\partial B_z}{\partial y}B_y+\frac{\partial B_z}{\partial x}B_x \end{bmatrix}-\begin{bmatrix} \frac{\partial B_y}{\partial x}B_y+\frac{\partial B_z}{\partial x}B_z \\ \frac{\partial B_x}{\partial y}B_x+\frac{\partial B_z}{\partial y}B_z \\ \frac{\partial B_x}{\partial z}B_x+\frac{\partial B_y}{\partial z}B_y \end{bmatrix}$$

$$=\begin{bmatrix} \frac{\partial B_x}{\partial x}B_x+\frac{\partial B_x}{\partial y}B_y+\frac{\partial B_x}{\partial z}B_z \\ \frac{\partial B_y}{\partial x}B_x+\frac{\partial B_y}{\partial y}B_y+\frac{\partial B_y}{\partial z}B_z \\ \frac{\partial B_z}{\partial x}B_x+\frac{\partial B_z}{\partial y}B_y+\frac{\partial B_z}{\partial z}B_z \end{bmatrix}$$

$$-\begin{bmatrix} \frac{\partial B_x}{\partial x}B_x+\frac{\partial B_y}{\partial x}B_y+\frac{\partial B_z}{\partial x}B_z \\ \frac{\partial B_x}{\partial y}B_x+\frac{\partial B_y}{\partial y}B_y+\frac{\partial B_z}{\partial y}B_z \\ \frac{\partial B_x}{\partial z}B_x+\frac{\partial B_y}{\partial z}B_y+\frac{\partial B_z}{\partial z}B_z \end{bmatrix}$$

$$=\begin{bmatrix} \left(B_x\frac{\partial}{\partial x}+B_y\frac{\partial}{\partial y}+B_z\frac{\partial}{\partial z}\right)B_x \\ \left(B_x\frac{\partial}{\partial x}+B_y\frac{\partial}{\partial y}+B_z\frac{\partial}{\partial z}\right)B_y \\ \left(B_x\frac{\partial}{\partial x}+B_y\frac{\partial}{\partial y}+B_z\frac{\partial}{\partial z}\right)B_z \end{bmatrix}$$

$$-\frac{1}{2}\begin{bmatrix} \frac{\partial\left(B_x^2+B_y^2+B_z^2\right)}{\partial x} \\ \frac{\partial\left(B_x^2+B_y^2+B_z^2\right)}{\partial y} \\ \frac{\partial\left(B_x^2+B_y^2+B_z^2\right)}{\partial z} \end{bmatrix}$$

$$=(\mathbf{B}\cdot\nabla)\mathbf{B}-\frac{1}{2}\nabla|\mathbf{B}|^2$$

Theorem (4): *Maxwell Stress Tensor in Rectangular Coordinates*

In rectangular coordinates, the following vector field can be rewritten as the divergence of a tensor field

$$(\nabla\times\mathbf{B})\times\mathbf{B}+(\nabla\cdot\mathbf{B})\mathbf{B}=$$

$$\nabla\cdot\left(\begin{bmatrix} B_xB_x & B_xB_y & B_xB_z \\ B_yB_x & B_yB_y & B_yB_z \\ B_zB_x & B_zB_y & B_zB_z \end{bmatrix}-\frac{1}{2}|\mathbf{B}|^2\begin{bmatrix} 1 & 0 & 0 \\ 0 & 1 & 0 \\ 0 & 0 & 1 \end{bmatrix}\right) \tag{96}$$

Proof:

$$(\nabla\times\mathbf{B})\times\mathbf{B}+(\nabla\cdot\mathbf{B})\mathbf{B}$$

$$=\begin{bmatrix} \frac{\partial B_z}{\partial y}-\frac{\partial B_y}{\partial z} \\ \frac{\partial B_x}{\partial z}-\frac{\partial B_z}{\partial x} \\ \frac{\partial B_y}{\partial x}-\frac{\partial B_x}{\partial y} \end{bmatrix}\times\begin{bmatrix} B_x \\ B_y \\ B_z \end{bmatrix}+\left(\frac{\partial B_x}{\partial x}+\frac{\partial B_y}{\partial y}+\frac{\partial B_z}{\partial z}\right)\begin{bmatrix} B_x \\ B_y \\ B_z \end{bmatrix}$$

$$
=\begin{bmatrix}
\left(\frac{\partial B_x}{\partial z}-\frac{\partial B_z}{\partial x}\right)B_z-\left(\frac{\partial B_y}{\partial x}-\frac{\partial B_x}{\partial y}\right)B_y\\
\left(\frac{\partial B_y}{\partial x}-\frac{\partial B_x}{\partial y}\right)B_x-\left(\frac{\partial B_z}{\partial y}-\frac{\partial B_y}{\partial z}\right)B_z\\
\left(\frac{\partial B_z}{\partial y}-\frac{\partial B_y}{\partial z}\right)B_y-\left(\frac{\partial B_x}{\partial z}-\frac{\partial B_z}{\partial x}\right)B_x
\end{bmatrix}
$$

$$
+\begin{bmatrix}
\left(\frac{\partial B_x}{\partial x}+\frac{\partial B_y}{\partial y}+\frac{\partial B_z}{\partial z}\right)B_x\\
\left(\frac{\partial B_x}{\partial x}+\frac{\partial B_y}{\partial y}+\frac{\partial B_z}{\partial z}\right)B_y\\
\left(\frac{\partial B_x}{\partial x}+\frac{\partial B_y}{\partial y}+\frac{\partial B_z}{\partial z}\right)B_z
\end{bmatrix}
$$

$$
=\begin{bmatrix}
\left(\frac{\partial B_y}{\partial y}B_x+B_y\frac{\partial B_x}{\partial y}\right)+\left(\frac{\partial B_x}{\partial z}B_z+B_x\frac{\partial B_z}{\partial z}\right)\\
\left(\frac{\partial B_y}{\partial x}B_x+B_y\frac{\partial B_x}{\partial x}\right)+\left(\frac{\partial B_y}{\partial z}B_z+B_y\frac{\partial B_z}{\partial z}\right)\\
\left(\frac{\partial B_z}{\partial x}B_x+B_z\frac{\partial B_x}{\partial x}\right)+\left(\frac{\partial B_z}{\partial y}B_y+B_z\frac{\partial B_y}{\partial y}\right)
\end{bmatrix}
$$

$$
+\begin{bmatrix}
\left(\frac{\partial B_x}{\partial x}B_x-\frac{\partial B_y}{\partial x}B_y-\frac{\partial B_z}{\partial x}B_z\right)\\
\left(\frac{\partial B_y}{\partial y}B_y-\frac{\partial B_x}{\partial y}B_x-\frac{\partial B_z}{\partial y}B_z\right)\\
\left(\frac{\partial B_z}{\partial z}B_z-\frac{\partial B_x}{\partial z}B_x-\frac{\partial B_y}{\partial z}B_y\right)
\end{bmatrix}
$$

$$
=\begin{bmatrix}
\frac{\partial(B_yB_x)}{\partial y}+\frac{\partial(B_zB_x)}{\partial z}\\
\frac{\partial(B_xB_y)}{\partial x}+\frac{\partial(B_zB_y)}{\partial z}\\
\frac{\partial(B_xB_z)}{\partial x}+\frac{\partial(B_yB_z)}{\partial y}
\end{bmatrix}
+\begin{bmatrix}
\frac{1}{2}\frac{\partial\left(B_x^{\,2}-B_y^{\,2}-B_z^{\,2}\right)}{\partial x}\\
\frac{1}{2}\frac{\partial\left(B_y^{\,2}-B_x^{\,2}-B_z^{\,2}\right)}{\partial y}\\
\frac{1}{2}\frac{\partial\left(B_z^{\,2}-B_x^{\,2}-B_y^{\,2}\right)}{\partial z}
\end{bmatrix}
$$

$$
=\begin{bmatrix}
\frac{\partial(B_yB_x)}{\partial y}+\frac{\partial(B_zB_x)}{\partial z}\\
\frac{\partial(B_xB_y)}{\partial x}+\frac{\partial(B_zB_y)}{\partial z}\\
\frac{\partial(B_xB_z)}{\partial x}+\frac{\partial(B_yB_z)}{\partial y}
\end{bmatrix}
+\begin{bmatrix}
\frac{\partial}{\partial x}\left(B_x^{\,2}-\frac{1}{2}|\mathbf{B}|^2\right)\\
\frac{\partial}{\partial y}\left(B_y^{\,2}-\frac{1}{2}|\mathbf{B}|^2\right)\\
\frac{\partial}{\partial z}\left(B_z^{\,2}-\frac{1}{2}|\mathbf{B}|^2\right)
\end{bmatrix}
$$

$$
=\begin{bmatrix}
\nabla\cdot\left(\left(B_x^{\,2}-\frac{1}{2}|\mathbf{B}|^2\right)\mathbf{a}_x+(B_yB_x)\mathbf{a}_y+(B_zB_x)\mathbf{a}_z\right)\\
\nabla\cdot\left((B_xB_y)\mathbf{a}_x+\left(B_y^{\,2}-\frac{1}{2}|\mathbf{B}|^2\right)\mathbf{a}_y+(B_zB_y)\mathbf{a}_z\right)\\
\nabla\cdot\left((B_xB_z)\mathbf{a}_x+(B_yB_z)\mathbf{a}_y+\left(B_z^{\,2}-\frac{1}{2}|\mathbf{B}|^2\right)\mathbf{a}_z\right)
\end{bmatrix}
$$

Each component of the above vector (which is a scalar) has been written in the form of the divergence of a vector. All three vectors can be collected in a tensor where each column of the below tensor represents each of the above vectors.

$$
=\nabla\cdot\left(\begin{bmatrix}B_xB_x & B_xB_y & B_xB_z\\ B_yB_x & B_yB_y & B_yB_z\\ B_zB_x & B_zB_y & B_zB_z\end{bmatrix}-\frac{1}{2}|\mathbf{B}|^2\begin{bmatrix}1&0&0\\0&1&0\\0&0&1\end{bmatrix}\right)
$$

Theorem (5): *Making effort to Derive Maxwell Stress Tensor in Cylindrical Coordinates*

In Theorem (4), if the subscripts of (x,y,z) are changed to (r,θ,z) to represent cylindrical coordinates, then the resulting expression would be invalid, and a few extra terms must appear to compensate the error,

$$
(\nabla\times\mathbf{B})\times\mathbf{B}+(\nabla\cdot\mathbf{B})\mathbf{B}=
\nabla\cdot\left(\begin{bmatrix}B_rB_r & B_rB_\theta & B_zB_r\\ B_\theta B_r & B_\theta B_\theta & B_\theta B_z\\ B_zB_r & B_zB_\theta & B_zB_z\end{bmatrix}-\frac{1}{2}|\mathbf{B}|^2\begin{bmatrix}1&0&0\\0&1&0\\0&0&1\end{bmatrix}\right)
+\begin{bmatrix}\frac{1}{r}\frac{1}{2}\left(B_r^{\,2}-B_\theta^{\,2}+B_z^{\,2}\right)\\ \frac{1}{r}(B_rB_\theta)\\ 0\end{bmatrix}
\tag{97}
$$

In many engineering papers [5], the last vector term is dropped because of the mistaken impression that the Maxwell stress tensor is coordinate-independent.

Proof:

$$
(\nabla\times\mathbf{B})\times\mathbf{B}+(\nabla\cdot\mathbf{B})\mathbf{B}
$$

$$
=\begin{bmatrix}
\frac{1}{r}\frac{\partial B_z}{\partial\theta}-\frac{\partial B_\theta}{\partial z}\\
\frac{\partial B_r}{\partial z}-\frac{\partial B_z}{\partial r}\\
\left(\frac{1}{r}+\frac{\partial}{\partial r}\right)B_\theta-\frac{1}{r}\frac{\partial B_r}{\partial\theta}
\end{bmatrix}\times\begin{bmatrix}B_r\\B_\theta\\B_z\end{bmatrix}
$$

$$
+\left(\left(\frac{1}{r}+\frac{\partial}{\partial r}\right)B_r+\frac{1}{r}\frac{\partial B_\theta}{\partial\theta}+\frac{\partial B_z}{\partial z}\right)\begin{bmatrix}B_r\\B_\theta\\B_z\end{bmatrix}
$$

$$
=\begin{bmatrix}
\left(\frac{\partial B_r}{\partial z}-\frac{\partial B_z}{\partial r}\right)B_z-\left(\left(\frac{1}{r}+\frac{\partial}{\partial r}\right)B_\theta-\frac{1}{r}\frac{\partial B_r}{\partial\theta}\right)B_\theta\\
\left(\left(\frac{1}{r}+\frac{\partial}{\partial r}\right)B_\theta-\frac{1}{r}\frac{\partial B_r}{\partial\theta}\right)B_r-\left(\frac{1}{r}\frac{\partial B_z}{\partial\theta}-\frac{\partial B_\theta}{\partial z}\right)B_z\\
\left(\frac{1}{r}\frac{\partial B_z}{\partial\theta}-\frac{\partial B_\theta}{\partial z}\right)B_\theta-\left(\frac{\partial B_r}{\partial z}-\frac{\partial B_z}{\partial r}\right)B_r
\end{bmatrix}
$$

$$+\begin{bmatrix}\left(\left(\frac{1}{r}+\frac{\partial}{\partial r}\right)B_r+\frac{1}{r}\frac{\partial B_\theta}{\partial\theta}+\frac{\partial B_z}{\partial z}\right)B_r\\ \left(\left(\frac{1}{r}+\frac{\partial}{\partial r}\right)B_r+\frac{1}{r}\frac{\partial B_\theta}{\partial\theta}+\frac{\partial B_z}{\partial z}\right)B_\theta\\ \left(\left(\frac{1}{r}+\frac{\partial}{\partial r}\right)B_r+\frac{1}{r}\frac{\partial B_\theta}{\partial\theta}+\frac{\partial B_z}{\partial z}\right)B_z\end{bmatrix}$$

$$=\begin{bmatrix}\left(B_r\left(\frac{1}{r}+\frac{\partial}{\partial r}\right)B_r-B_\theta\left(\frac{1}{r}+\frac{\partial}{\partial r}\right)B_\theta-\frac{\partial B_z}{\partial r}B_z\right)\\ \left(\frac{1}{r}\frac{\partial B_\theta}{\partial\theta}B_\theta-\frac{1}{r}\frac{\partial B_r}{\partial\theta}B_r-\frac{1}{r}\frac{\partial B_z}{\partial\theta}B_z\right)\\ \left(B_z\frac{\partial B_z}{\partial z}-\frac{\partial B_\theta}{\partial z}B_\theta-\frac{\partial B_r}{\partial z}B_r\right)\end{bmatrix}$$

$$+\begin{bmatrix}\left(\frac{1}{r}\frac{\partial B_r}{\partial\theta}B_\theta+\frac{1}{r}\frac{\partial B_\theta}{\partial\theta}B_r\right)\\ \left(B_r\left(\frac{1}{r}+\frac{\partial}{\partial r}\right)B_\theta+B_\theta\left(\frac{1}{r}+\frac{\partial}{\partial r}\right)B_r\right)\\ \left(\frac{\partial B_z}{\partial r}B_r+B_z\left(\frac{1}{r}+\frac{\partial}{\partial r}\right)B_r\right)\end{bmatrix}$$

$$+\begin{bmatrix}\left(\frac{\partial B_z}{\partial z}B_r+\frac{\partial B_r}{\partial z}B_z\right)\\ \left(\frac{\partial B_\theta}{\partial z}B_z+\frac{\partial B_z}{\partial z}B_\theta\right)\\ \left(\frac{1}{r}\frac{\partial B_z}{\partial\theta}B_\theta+B_z\frac{1}{r}\frac{\partial B_\theta}{\partial\theta}\right)\end{bmatrix}$$

$$=\begin{bmatrix}\left(\frac{1}{r}\left(B_r^2-B_\theta^2\right)+\frac{1}{2}\frac{\partial\left(B_r^2-B_\theta^2-B_z^2\right)}{\partial r}\right)\\ \frac{1}{2}\frac{1}{r}\frac{\partial\left(B_\theta^2-B_r^2-B_z^2\right)}{\partial\theta}\\ \frac{1}{2}\frac{\partial\left(B_z^2-B_r^2-B_\theta^2\right)}{\partial z}\end{bmatrix}$$

$$+\begin{bmatrix}\frac{1}{r}\frac{\partial(B_\theta B_r)}{\partial\theta}+\frac{\partial(B_z B_r)}{\partial z}\\ \left(\frac{2}{r}+\frac{\partial}{\partial r}\right)(B_r B_\theta)+\frac{\partial(B_z B_\theta)}{\partial z}\\ \left(\frac{1}{r}+\frac{\partial}{\partial r}\right)(B_z B_r)+\frac{1}{r}\frac{\partial(B_\theta B_z)}{\partial\theta}\end{bmatrix}$$

$$=\begin{bmatrix}\frac{1}{r}\frac{1}{2}\left(B_r^2-B_\theta^2+B_z^2\right)\\ \frac{1}{r}(B_r B_\theta)\\ 0\end{bmatrix}$$

$$\begin{bmatrix}\frac{1}{2}\left(\frac{1}{r}+\frac{\partial}{\partial r}\right)\left(B_r^2-B_\theta^2-B_z^2\right)\\ \frac{1}{2}\frac{1}{r}\frac{\partial\left(B_\theta^2-B_r^2-B_z^2\right)}{\partial\theta}\\ \frac{1}{2}\frac{\partial\left(B_z^2-B_r^2-B_\theta^2\right)}{\partial z}\end{bmatrix}$$

$$+\begin{bmatrix}\frac{1}{r}\frac{\partial(B_\theta B_r)}{\partial\theta}+\frac{\partial(B_z B_r)}{\partial z}\\ \left(\frac{1}{r}+\frac{\partial}{\partial r}\right)(B_r B_\theta)+\frac{\partial(B_z B_\theta)}{\partial z}\\ \left(\frac{1}{r}+\frac{\partial}{\partial r}\right)(B_z B_r)+\frac{1}{r}\frac{\partial(B_\theta B_z)}{\partial\theta}\end{bmatrix}$$

$$=\begin{bmatrix}\frac{1}{r}\frac{1}{2}\left(B_r^2-B_\theta^2+B_z^2\right)\\ \frac{1}{r}(B_r B_\theta)\\ 0\end{bmatrix}$$

$$\begin{bmatrix}\nabla\cdot\left(\frac{1}{2}\left(B_r^2-B_\theta^2-B_z^2\right)\mathbf{a}_r+(B_\theta B_r)\mathbf{a}_\theta+(B_z B_r)\mathbf{a}_z\right)\\ \nabla\cdot\left((B_r B_\theta)\mathbf{a}_r+\frac{1}{2}\left(B_\theta^2-B_r^2-B_z^2\right)\mathbf{a}_\theta+(B_z B_\theta)\mathbf{a}_z\right)\\ \nabla\cdot\left((B_z B_r)\mathbf{a}_r+(B_\theta B_z)\mathbf{a}_\theta+\frac{1}{2}\left(B_z^2-B_r^2-B_\theta^2\right)\mathbf{a}_z\right)\end{bmatrix}$$

Theorem (6): *Couple Stress Vector*

In cylindrical coordinates, the following scalar field can be written as the divergence of a vector field,

$$r\left((\nabla\times\mathbf{B})\times\mathbf{B}+(\nabla\cdot\mathbf{B})\mathbf{B}\right)_\theta=\nabla\cdot r\begin{bmatrix}B_r B_\theta\\ B_\theta^2-\frac{1}{2}|\mathbf{B}|^2\\ B_z B_\theta\end{bmatrix}\qquad(98)$$

Proof:

From the last Theorem, the force density in cylindrical coordinates was obtained as follows,

$$(\nabla\times\mathbf{B})\times\mathbf{B}+(\nabla\cdot\mathbf{B})\mathbf{B}=$$

$$\nabla\cdot\left(\begin{bmatrix}B_r B_r & B_r B_\theta & B_z B_r\\ B_\theta B_r & B_\theta B_\theta & B_\theta B_z\\ B_z B_r & B_z B_\theta & B_z B_z\end{bmatrix}-\frac{1}{2}|\mathbf{B}|^2\begin{bmatrix}1&0&0\\0&1&0\\0&0&1\end{bmatrix}\right)$$

$$+\begin{bmatrix}\frac{1}{r}\frac{1}{2}\left(B_r^2-B_\theta^2+B_z^2\right)\\ \frac{1}{r}(B_r B_\theta)\\ 0\end{bmatrix}$$

i.e. not completely as the divergence of a vector field. the tangential component is extracted as,

$$((\nabla \times \mathbf{B}) \times \mathbf{B} + (\nabla \cdot \mathbf{B})\mathbf{B})_\theta$$

$$= \frac{1}{r}(B_r B_\theta) + \nabla \cdot \begin{bmatrix} B_r B_\theta \\ B_\theta^{\ 2} - \frac{1}{2}|\mathbf{B}|^2 \\ B_z B_\theta \end{bmatrix}$$

Multiplying the tangential component by r,

$$r((\nabla \times \mathbf{B}) \times \mathbf{B} + (\nabla \cdot \mathbf{B})\mathbf{B})_\theta$$

$$= (B_r B_\theta) + r\nabla \cdot \begin{bmatrix} B_r B_\theta \\ B_\theta^{\ 2} - \frac{1}{2}|\mathbf{B}|^2 \\ B_z B_\theta \end{bmatrix}$$

Or equivalently,

$$= \mathbf{a}_r \cdot \begin{bmatrix} B_r B_\theta \\ B_\theta^{\ 2} - \frac{1}{2}|\mathbf{B}|^2 \\ B_z B_\theta \end{bmatrix} + r\nabla \cdot \begin{bmatrix} B_r B_\theta \\ B_\theta^{\ 2} - \frac{1}{2}|\mathbf{B}|^2 \\ B_z B_\theta \end{bmatrix}$$

where $\mathbf{a}_r$ is the unit radial vector.
On the other hand, It is easy to show that $\nabla r = \mathbf{a}_r$,

$$= \nabla r \cdot \begin{bmatrix} B_r B_\theta \\ B_\theta^{\ 2} - \frac{1}{2}|\mathbf{B}|^2 \\ B_z B_\theta \end{bmatrix} + r\nabla \cdot \begin{bmatrix} B_r B_\theta \\ B_\theta^{\ 2} - \frac{1}{2}|\mathbf{B}|^2 \\ B_z B_\theta \end{bmatrix}$$

The above equation is in the expanded form of the divergence of the product of a scalar field (f) and a vector field ($\mathbf{F}$),

$$\nabla f \cdot \mathbf{F} + f\nabla \cdot \mathbf{F} = \nabla \cdot (f\mathbf{F})$$

Application of the above product rule completes the proof.

Theorem (7): *Maxwell Stress Tensor in Cylindrical Coordinates*

$$(\nabla \times \mathbf{B}) \times \mathbf{B} + (\nabla \cdot \mathbf{B})\mathbf{B} = \nabla \cdot \begin{bmatrix} T_{xr} & T_{x\theta} & T_{xz} \\ T_{yr} & T_{y\theta} & T_{yz} \\ T_{zr} & T_{z\theta} & T_{zz} \end{bmatrix} \tag{99}$$

$$T_{xr} = \frac{1}{2}\cos(\theta)\left(B_r^{\ 2} - B_\theta^{\ 2} - B_z^{\ 2}\right) - \sin(\theta) B_r B_\theta$$

$$T_{x\theta} = \frac{1}{2}\sin(\theta)\left(B_r^{\ 2} - B_\theta^{\ 2} + B_z^{\ 2}\right) + \cos(\theta) B_r B_\theta$$

$$T_{xz} = \cos(\theta) B_r - \sin(\theta) B_\theta B_z$$

$$T_{yr} = \frac{1}{2}\sin(\theta)\left(B_r^{\ 2} - B_\theta^{\ 2} - B_z^{\ 2}\right) + \cos(\theta) B_r B_\theta$$

$$T_{y\theta} = \frac{1}{2}\cos(\theta)\left(B_\theta^{\ 2} - B_r^{\ 2} - B_z^{\ 2}\right) + \sin(\theta) B_r B_\theta$$

$$T_{yz} = \cos(\theta) B_\theta + \sin(\theta) B_r B_z$$

$$T_{zr} = B_r B_z$$

$$T_{z\theta} = B_\theta B_z$$

$$T_{zz} = \frac{1}{2}\left(B_z^{\ 2} - B_r^{\ 2} - B_\theta^{\ 2}\right)$$

Proof:
Since (96) is a collection of three vector fields (each row), each one can be expressed in cylindrical coordinates. To this end, the following coordinate system transformation can be employed,

$$i \in \{1,2,3\}: \begin{bmatrix} T_{ir} \\ T_{i\theta} \\ T_{iz} \end{bmatrix} = \begin{bmatrix} \cos(\theta) & \sin(\theta) & 0 \\ -\sin(\theta) & \cos(\theta) & 0 \\ 0 & 0 & 1 \end{bmatrix} \begin{bmatrix} T_{ix} \\ T_{iy} \\ T_{iz} \end{bmatrix} \tag{100}$$

where $i \in \{x,y,z\}$,

$$\begin{bmatrix} B_x \\ B_y \\ B_z \end{bmatrix} = \begin{bmatrix} \cos(\theta) & -\sin(\theta) & 0 \\ \sin(\theta) & \cos(\theta) & 0 \\ 0 & 0 & 1 \end{bmatrix} \begin{bmatrix} B_r \\ B_\theta \\ B_z \end{bmatrix} \tag{101}$$

Substituting (101) in (96) and the resulting expression in (100) yields (99).

Remark: The usage of the Maxwell stress tensor in cylindrical coordinates is facilitation of computation. For instance, for the calculation of the resultant force on the rotor, the surface of integration becomes a cylindrical shell. It is stressed that the surface integration of the Maxwell stress tensor still yields the resultant force in rectangular coordinates.

$$F_i = \mu_0^{-1} \int_S \left(T_{ir}\mathbf{a}_r + T_{i\theta}\mathbf{a}_\theta + T_{iz}\mathbf{a}_z\right) \cdot d\mathbf{s}$$

where $i \in \{x,y,z\}$.

Theorem (8): *Maxwell Couple Stress Tensor in terms of Maxwell Stress Tensor*

$$\mathbf{r} \times (\nabla \cdot \boldsymbol{\sigma})$$

$$\nabla \cdot \begin{bmatrix} (\mathbf{r} \times \boldsymbol{\sigma}_x)_x & (\mathbf{r} \times \boldsymbol{\sigma}_y)_x & (\mathbf{r} \times \boldsymbol{\sigma}_z)_x \\ (\mathbf{r} \times \boldsymbol{\sigma}_x)_y & (\mathbf{r} \times \boldsymbol{\sigma}_y)_y & (\mathbf{r} \times \boldsymbol{\sigma}_z)_y \\ (\mathbf{r} \times \boldsymbol{\sigma}_x)_z & (\mathbf{r} \times \boldsymbol{\sigma}_y)_z & (\mathbf{r} \times \boldsymbol{\sigma}_z)_z \end{bmatrix} \tag{102}$$

where

$$\boldsymbol{\sigma} = \begin{bmatrix} \boldsymbol{\sigma}_x^{\ T} \\ \boldsymbol{\sigma}_y^{\ T} \\ \boldsymbol{\sigma}_z^{\ T} \end{bmatrix} = \begin{bmatrix} \sigma_{xx} & \sigma_{xy} & \sigma_{xz} \\ \sigma_{yx} & \sigma_{yy} & \sigma_{yz} \\ \sigma_{zx} & \sigma_{zy} & \sigma_{zz} \end{bmatrix}$$

Proof:

$$\mathbf{r}\times(\nabla\cdot\boldsymbol{\sigma})=\begin{bmatrix}x\\y\\z\end{bmatrix}\times\begin{bmatrix}\frac{\partial\sigma_{xx}}{\partial x}+\frac{\partial\sigma_{xy}}{\partial y}+\frac{\partial\sigma_{xz}}{\partial z}\\ \frac{\partial\sigma_{yx}}{\partial x}+\frac{\partial\sigma_{yy}}{\partial y}+\frac{\partial\sigma_{yz}}{\partial z}\\ \frac{\partial\sigma_{zx}}{\partial x}+\frac{\partial\sigma_{zy}}{\partial y}+\frac{\partial\sigma_{zz}}{\partial z}\end{bmatrix}$$

$$=\begin{bmatrix}y\left(\frac{\partial\sigma_{zx}}{\partial x}+\frac{\partial\sigma_{zy}}{\partial y}+\frac{\partial\sigma_{zz}}{\partial z}\right)-z\left(\frac{\partial\sigma_{yx}}{\partial x}+\frac{\partial\sigma_{yy}}{\partial y}+\frac{\partial\sigma_{yz}}{\partial z}\right)\\ z\left(\frac{\partial\sigma_{xx}}{\partial x}+\frac{\partial\sigma_{xy}}{\partial y}+\frac{\partial\sigma_{xz}}{\partial z}\right)-x\left(\frac{\partial\sigma_{zx}}{\partial x}+\frac{\partial\sigma_{zy}}{\partial y}+\frac{\partial\sigma_{zz}}{\partial z}\right)\\ x\left(\frac{\partial\sigma_{yx}}{\partial x}+\frac{\partial\sigma_{yy}}{\partial y}+\frac{\partial\sigma_{yz}}{\partial z}\right)-y\left(\frac{\partial\sigma_{xx}}{\partial x}+\frac{\partial\sigma_{xy}}{\partial y}+\frac{\partial\sigma_{xz}}{\partial z}\right)\end{bmatrix}$$

By virtue of $\sigma_{ij}=\sigma_{ji}$, the symmetry of Maxwell stress tensor, the terms in the form of $\sigma_{ij}\partial j/\partial j-\sigma_{ji}\partial i/\partial i=0$ can be added and subtracted,

$$=\begin{bmatrix}\frac{\partial(y\sigma_{zx})}{\partial x}+\frac{\partial(y\sigma_{zz})}{\partial z}-\frac{\partial(z\sigma_{yx})}{\partial x}-\frac{\partial(z\sigma_{yy})}{\partial y}\\ \frac{\partial(z\sigma_{xx})}{\partial x}+\frac{\partial(z\sigma_{xy})}{\partial y}-\frac{\partial(x\sigma_{zy})}{\partial y}-\frac{\partial(x\sigma_{zz})}{\partial z}\\ \frac{\partial(x\sigma_{yy})}{\partial y}+\frac{\partial(x\sigma_{yz})}{\partial z}-\frac{\partial(y\sigma_{xx})}{\partial x}-\frac{\partial(y\sigma_{xz})}{\partial z}\end{bmatrix}$$

$$+\begin{bmatrix}y\frac{\partial\sigma_{zy}}{\partial y}+\frac{\partial y}{\partial y}\sigma_{zy}-\frac{\partial z}{\partial z}\sigma_{yz}-z\frac{\partial\sigma_{yz}}{\partial z}\\ z\frac{\partial\sigma_{xz}}{\partial z}+\frac{\partial z}{\partial z}\sigma_{xz}-\frac{\partial x}{\partial x}\sigma_{zx}-x\frac{\partial\sigma_{zx}}{\partial x}\\ x\frac{\partial\sigma_{yx}}{\partial x}+\frac{\partial x}{\partial x}\sigma_{yx}-\frac{\partial y}{\partial y}\sigma_{xy}-y\frac{\partial\sigma_{xy}}{\partial y}\end{bmatrix}$$

that allows expressing the vector as

$$=\begin{bmatrix}\frac{\partial(y\sigma_{zx}-z\sigma_{yx})}{\partial x}+\frac{\partial(y\sigma_{zy}-z\sigma_{yy})}{\partial y}+\frac{\partial(y\sigma_{zz}-z\sigma_{yz})}{\partial z}\\ \frac{\partial(z\sigma_{xx}-x\sigma_{zx})}{\partial x}+\frac{\partial(z\sigma_{xy}-x\sigma_{zy})}{\partial y}+\frac{\partial(z\sigma_{xz}-x\sigma_{zz})}{\partial z}\\ \frac{\partial(x\sigma_{yx}-y\sigma_{xx})}{\partial x}+\frac{\partial(x\sigma_{yy}-y\sigma_{xy})}{\partial y}+\frac{\partial(x\sigma_{yz}-y\sigma_{xz})}{\partial z}\end{bmatrix}$$

in the form of the divergence of a tensor field,

$$=\nabla\cdot\begin{bmatrix}y\sigma_{zx}-z\sigma_{yx} & y\sigma_{zy}-z\sigma_{yy} & y\sigma_{zz}-z\sigma_{yz}\\ z\sigma_{xx}-x\sigma_{zx} & z\sigma_{xy}-x\sigma_{zy} & z\sigma_{xz}-x\sigma_{zz}\\ x\sigma_{yx}-y\sigma_{xx} & x\sigma_{yy}-y\sigma_{xy} & x\sigma_{yz}-y\sigma_{xz}\end{bmatrix}=\nabla\cdot\mathbf{m}$$

Recalling the form of Maxwell stress tensor $\boldsymbol{\sigma}$,

$$\boldsymbol{\sigma}=\begin{bmatrix}\boldsymbol{\sigma}_x^{\ T}\\ \boldsymbol{\sigma}_y^{\ T}\\ \boldsymbol{\sigma}_z^{\ T}\end{bmatrix}=\begin{bmatrix}\sigma_{xx} & \sigma_{xy} & \sigma_{xz}\\ \sigma_{yx} & \sigma_{yy} & \sigma_{yz}\\ \sigma_{zx} & \sigma_{zy} & \sigma_{zz}\end{bmatrix}$$

the tensor $\mathbf{m}$ can be written in terms of the Maxwell stress tensor,

$$\mathbf{m}=\begin{bmatrix}(\mathbf{r}\times\boldsymbol{\sigma}_x)_x & (\mathbf{r}\times\boldsymbol{\sigma}_y)_x & (\mathbf{r}\times\boldsymbol{\sigma}_z)_x\\ (\mathbf{r}\times\boldsymbol{\sigma}_x)_y & (\mathbf{r}\times\boldsymbol{\sigma}_y)_y & (\mathbf{r}\times\boldsymbol{\sigma}_z)_y\\ (\mathbf{r}\times\boldsymbol{\sigma}_x)_z & (\mathbf{r}\times\boldsymbol{\sigma}_y)_z & (\mathbf{r}\times\boldsymbol{\sigma}_z)_z\end{bmatrix}$$